Gravity data acquisition and potential-field data modelling along Metal Earth's Chibougamau transect using geophysical and geological constraints

by

Amir Maleki Ghahfarokhi

A thesis submitted in partial fulfillment
of the requirement for the degree of
Master of Science (MSc) in Geology

The Faculty of Graduate Studies
Laurentian University
Sudbury, Ontario, Canada

© Amir Maleki Ghahfarokhi, 2019

THESIS DEFENCE COMMITTEE/COMITÉ DE SOUTENANCE DE THÈSE
Laurentian Université/Université Laurentienne
Faculty of Graduate Studies/Faculté des études supérieures

Title of Thesis Titre de la thèse	Gravity data acquisition and potential-field data modelling along Metal Earth's Chibougamau transect using geophysical and geological constraints
Name of Candidate Nom du candidat	Ghahfarokhi, Amir
Degree Diplôme	Master of Science
Department/Program Département/Programme	Geology
Date of Defence Date de la soutenance	July 26, 2019

APPROVED/APPROUVÉ

Thesis Examiners/Examinateurs de thèse:

Dr. Richard Smith
(Supervisor/Directeur de thèse)

Dr. Esmaeil Eshagi
(Committee member/Membre du comité)

Dr. Pierrick Altwegg
(Committee member/Membre du comité)

Dr. Hernan Ugalde
(External Examiner/Examinateur externe)

Approved for the Faculty of Graduate Studies
Approuvé pour la Faculté des études supérieures
Dr. David Lesbarrères
Monsieur David Lesbarrères
Dean, Faculty of Graduate Studies
Doyen, Faculté des études supérieures

ACCESSIBILITY CLAUSE AND PERMISSION TO USE

I, **Amir Ghahfarokhi**, hereby grant to Laurentian University and/or its agents the non-exclusive license to archive and make accessible my thesis, dissertation, or project report in whole or in part in all forms of media, now or for the duration of my copyright ownership. I retain all other ownership rights to the copyright of the thesis, dissertation or project report. I also reserve the right to use in future works (such as articles or books) all or part of this thesis, dissertation, or project report. I further agree that permission for copying of this thesis in any manner, in whole or in part, for scholarly purposes may be granted by the professor or professors who supervised my thesis work or, in their absence, by the Head of the Department in which my thesis work was done. It is understood that any copying or publication or use of this thesis or parts thereof for financial gain shall not be allowed without my written permission. It is also understood that this copy is being made available in this form by the authority of the copyright owner solely for the purpose of private study and research and may not be copied or reproduced except as permitted by the copyright laws without written authority from the copyright owner.

Abstract

The Metal Earth (ME) project aims to understand the underlying geological mechanisms that differentiate mineral endowments in Precambrian greenstone belts of the Canadian Shield. The ME project acquires and collates various geological and geophysical data along 13 transects to create valid models of subsurface features in order to identify components that contribute to the mineralization processes that result in mineral endowment.

In this thesis, gravity observation along ~128 line kilometers in the Chibougamau transect is considered. The acquired data were checked for quality, processed to calculate the complete Bouguer anomaly and combined with existing gravity data provided by the Geological Survey of Canada.

Gravity and compiled magnetic data were forward modelled along four sections and constrained by surficial geological observations, seismic sections, and petrophysical properties to estimate and improve the geometry and depth of plutonic bodies, and identifying the subsurface features such as dykes and faults. These improvements will help others to identify components that contribute to mineralising processes.

Keywords

Chibougamau, Metal Earth project, potential field, gravity, magnetic, 2.5-D, geological modelling, forward modelling

Acknowledgment

This thesis is the most important product of my MSc research work. It has been a challenging research project with about 8 months of field work during two summers that has enriched my life. This research work would not have been completed without the help and support of many people, therefore I wish to express my sincere appreciation to them all.

First of all, I would like to thank my thesis supervisor, Richard Smith, for believing in me, the fatherly support, patience and the valuable and promptly provided comments on my drafts and ideas. He took his time to listen and attend to most of the challenges I encountered during this research work; taught me the basics of exploration geophysical and research techniques; how to read scientific papers; how to write scientific statements that would not be provocative. I learned a lot of valuable things from you that will take me very far in life.

Secondly, I would like to thank the Metal Earth project which financially supports this research work.

Am also deeply grateful to Esmaeil Eshaghi and Pierrick Altwegg for their valuable suggestions and comments during gravity data acquisition, gravity and magnetic data processing.

William McNeice, Fabiano Della Justina, Brandon Hume, Tara Smith, and Kerri Campbell, thank you all for your help during two field season for gravity data acquisition.

Lucy Mathieu, thank you so much for providing me with valuable geological corrections and suggestions during the interpretation of the Metal Earth seismic section and geological modelling.

I would like to thank from David Snyder, Mostafa Naghizadeh for the seismic tips they suggested to me during the interpretation of the Metal Earth seismic section.

My appreciation goes to Alan King, and all the geophysics research students, our weekly interactions at the departmental project-progress meetings were very valuable. Thank you.

I would like to thank from John Ayer for providing me valuable geological papers and reports.

To my parents, brother and sister, thank you all for your emotional supports and prayers from a long distance. Be happy and safe.

TABLE OF CONTENTS

List of Figures

List of Tables

Table Page

CHAPTER 1

1 Introduction to Thesis

1.1 Introduction

This chapter provides a brief overview of the regional geological setting of the Chibougamau area that is the focus of this study and the research problems that the thesis will address.

1.2 Geological setting

The Chibougamau area is located in the northeast corner of the Abitibi Subprovince (Figure 1-1) and bordered on the south-east by the Grenville province. The Archean rocks along the contact between the Superior and Grenville provinces were effected during the Grenvillian orogeny (1100- 970 Ma; Rivers et al. 1989; Baker 1980).

The main geological feature of the area is the Matagami-Chibougamau belt which trends east-west and terminates along the Grenville Front tectonic zone (Wynne-Edwards 1972; Rivers and Chown 1986). This belt has metamorphosed to amphibolite facies in the vicinity of the Grenville Front, and there are greenschist facies rocks in the rest of the area except around the intrusions, where amphibolite grades are observed.

In the Chibougamau area, abundant large granitoid plutons, made up mostly of tonalitic gneiss and tonalitic to dioritic plutons (Percival and Krogh 1983), have an important role in the northern portion of the Abitibi Subprovince, as they influence the attitude of the tectonic fabric (Racicot et al. 1984).

There are four distinct deformation events in the Matagami-Chibougamau belt. The first three (D1 to D3) are Archean in age and seem to be contemporaneous with and/or slightly younger than the emplacement of the Chibougamau Pluton, dated at 2717±2 Ma (Krogh 1982). The first phase (D1) formed folds with north-south fold axes, and the second phase (D2) generated prominent structures in the area including metamorphism, foliation, ductile faults and folds with east-west trending fold axes. The D3 deformation phase resulted in minor late faulting. The final deformation (D4), which is Proterozoic in age and limited to the belt near the Grenville Front is due to the Grenville orogeny.

The folds produced during the D2 regional deformation (Figure 1-1), are described from the north to the south as follows (Daigneault et al. 1990) (Figure 1-2):

(i) The Waconichi syncline (WS), the northern most structure, is made of sedimentary rocks of the Opémisca Group, which is bordered by longitudinal east-west faults (marked WS on Figure 1-1).

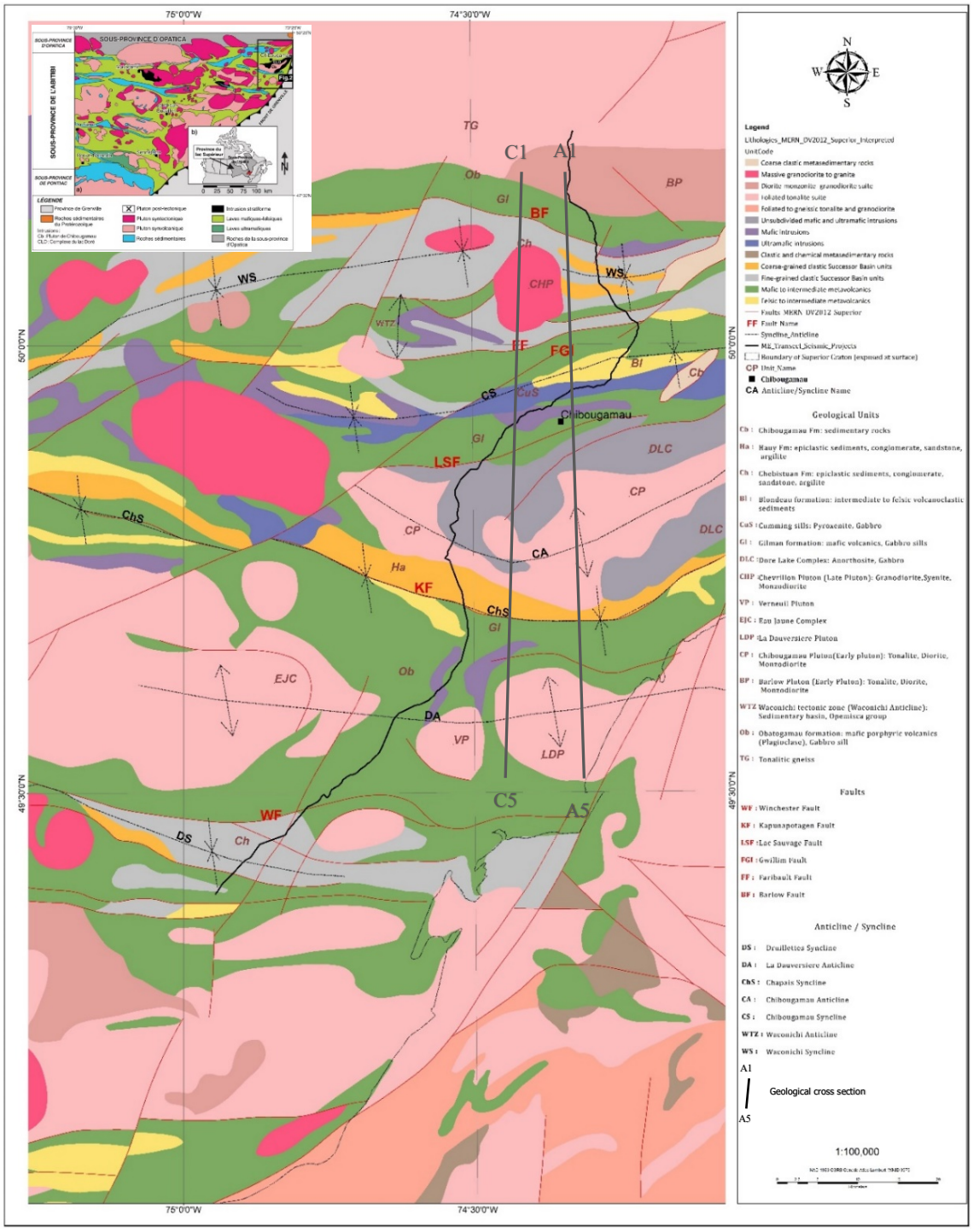

Figure 1-1. Geological map of the Chibougamau area, showing the distribution of the folds produced during the D2 regional deformation. The locations of two detailed cross-sections (A1-A5 and C1-C5; see Fig. 1-2) are denoted by thick straight black lines. Modified after Montsion et al. 2017, Daigneault et al. 1990, Leclerc et al. 2008

(ii) The Waconichi Anticline (WTZ): This presumed anticline is a tectonic amalgam lying between the Waconichi syncline and the Chibougamau syncline to its south. It consists of tectonic slices derived from various levels of the stratigraphic column. The southern limit of the WTZ is the Faribault fault (Daigneault 1982; Daigneault and Allard 1983, 1984).

(iii) The Chibougamau syncline (CS): The syncline outlined by the Cummings sills is composed of a series of subsidiary folds.

(iv) The Chibougamau anticline (CA): This anticlinal structure trends essentially east-west in the western portion but changes to northeast toward the eastern portion of the study area. It may be responsible for the doming volcanic pile of the Roy Group (Gobeil and Racicot 1983). The Lac Doré Complex (LDC) and Chibougamau pluton are the intrusions which make up the core of this anticline.

(v) The Chapais syncline (ChS): Like the Waconichi syncline, the Chapais syncline comprises sedimentary rocks of the Opemisca Group. Both the Cummings sills and the Blondeau Formation underly the sedimentary rocks. The ChS is bordered on the south by the Kapunapotagen fault (Charbonneau et al. 1983; Daigneault and Allard 1983, 1987).

(vi) The La Dauversière anticline (DA) is made of several granitoid plutons such as the Lapparent massif, the Eau Jaune Complex, the La Dauversière Pluton, the Boisvert, and some smaller intrusions. These plutons are believed to have emplaced in this anticline during early to late-tectonic phases in the regional deformation.

(vii) The Druillettes syncline (DS) is occupied by sedimentary rocks of the Caopatina Formation and is bounded by east-west striking longitudinal faults (Sharma et al. 1987).

Figure 1-3 shows a schematic cross section of the large synclinorium of the Chibougamau area.

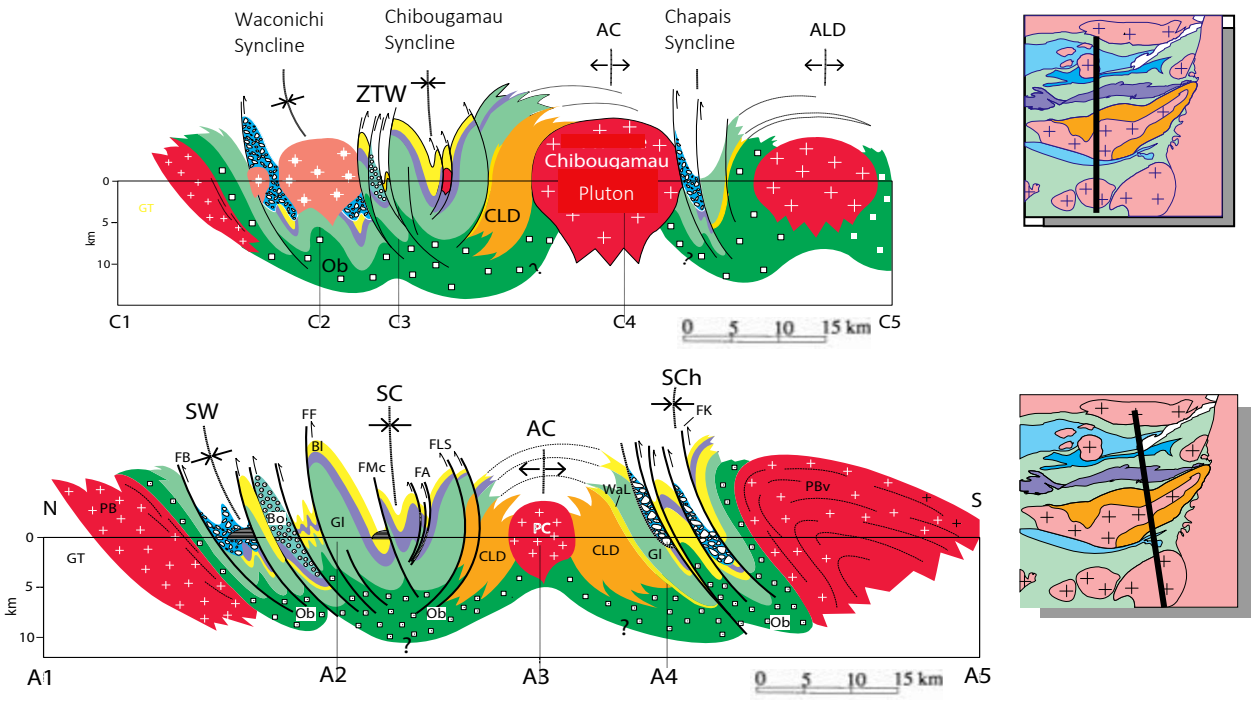

Figure 1-2. Detailed cross-section of the Chibougamau area. The top panel is section C1-C5 and the bottom panel is section A1-A5. See the legend of Figure 1-1 for abbreviations and the location of the cross sections (after Daigneault et al. 1990).

The system of large regional breaks known throughout the Abitibi subprovince, which in the Chibougamau area are predominantly east-west (e.g. the WTZ), have caused a repetition of the stratigraphic sequence (Daigneault and Allard 1987).

There are two examples of subvertical east-west faults which were active after D2 folding and that separate sedimentary rocks from earlier volcanic rocks. (i) In the CS, the Kapunapotagen fault is a thrust that uplift material from south to north (Charbonneau et al. 1983; Daigneault and Allard 1984), and (ii) in the WTZ, the Faribault fault is a north verging thrust (Daigneault and Allard 1983, 1984, 1987). However, there are geological issues as the repetition of the Lac Doré Complex and the Cummings Sills caused by the Lac Sauvage fault zone and the Lac Ailtoinette fault zone requires that thrusting must be north over the south.

There are two main intrusive events in the Chibougamau greenstone belt. (i) Pre- to syn-tectonic intrusions such as the La Dauversière pluton, dated at 2719,8 +3.0/-0.6 Ma (Mortensen 1993), which occupy the same stratigraphic level as the host rock, have caused doming of the strata, and (ii) post-regional intrusions such as the Chevrillon pluton, dated at 2693.1±1.7 Ma (unpublished age by M. Hamilton, University of Toronto, 2018) and Muscocho pluton, dated at 2701.2 +1.7/-1.3 Ma (Mortensen 1993) emplaced after or toward the end of the regional deformation and in near-vertical strata which could not reverse the host strata. It is possible that for some intrusions such as the Boisvert Pluton, La Dauversière Pluton, and the Eau Jaune Complex, which are aligned in an east-west direction, the emplacement of magma may be controlled by deep east-west fractures (Pitcher 1979; Castro 1986).

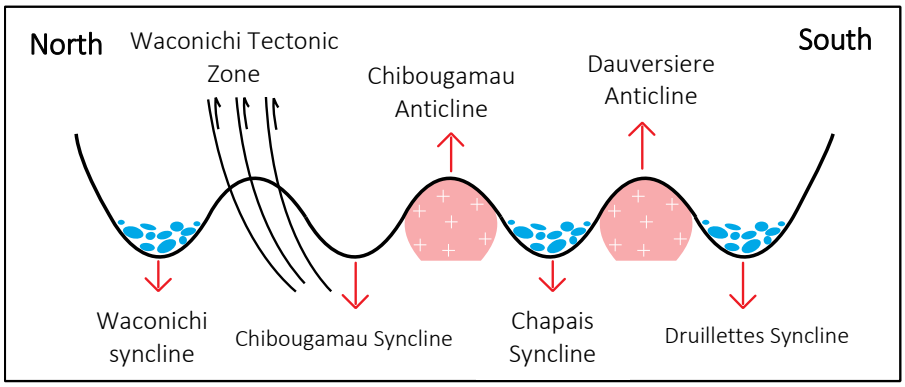

Figure 1-3. Schematic cross-section of the Chibougamau area, showing a large synclinorium consisting of four major synclines and three anticlines (after Daigneault et al 1990).

1.3 Stratigraphy

The Chibougamau greenstone belt consists of two major lithological groups. The Roy Group consists of two mafic-to-felsic volcanic cycles that are made up of basaltic lavas and intermediate to felsic pyroclastic rocks. The Opemisca Group is dominantly sedimentary and unconformably overlies the Roy group (Allard 1976; Gobeil and Racicot 1983; Allard and

Gobeil 1984; Daigneault and Allard 1987). More details about these groups are described below and shown in Figure 1-4.

In the first volcanic cycle of the Roy group, the basal units are the Obatogamau Formation (3-4 km thick), which consists of porphyric basaltic flows. Conformably above this is the Waconichi Formation (800 m thick), which is comprised of felsic volcanic rocks and it contains the exhalative Lac Sauvage iron formation (thinly bedded siderite, pyrite, chert, and iron oxides) (Henry and Allard 1979).

The second volcanic cycle initiates with the emission of pillow basalts of the Bruneau Formation (3-4 km thick), which are overlain by the intermediate to felsic volcaniclastic rocks of the Blondeau Formation (2-3 km thick). This latter Formation is intruded, near its base, by the three mafic intrusions designated Cummings sills (Dimorth et al. 1983). A uniform sequence of volcanoclastic rocks lies at the top of the Roy Group representing the Bordeleau Formation and shows a transition into the Opemisca Group which include sandstones, siltstones, and polygenic conglomerates (Mueller and Dimroth 1984, 1986).

The Opémisca Group contains boulders from the local units – for example, the rocks located south of the Chibougamau pluton contains pebbles from the Chibougamau pluton and the LDC – this means that these intrusions were already eroding when the Opémisca Group formed. The contact between the sediments and the intrusions is unconformable.

There is a sequence in the south of the study area, where the Caopatina Formation, which consists of volcaniclastic and sedimentary rocks, overlies the Obatogamau Formation (Figure 1-5).

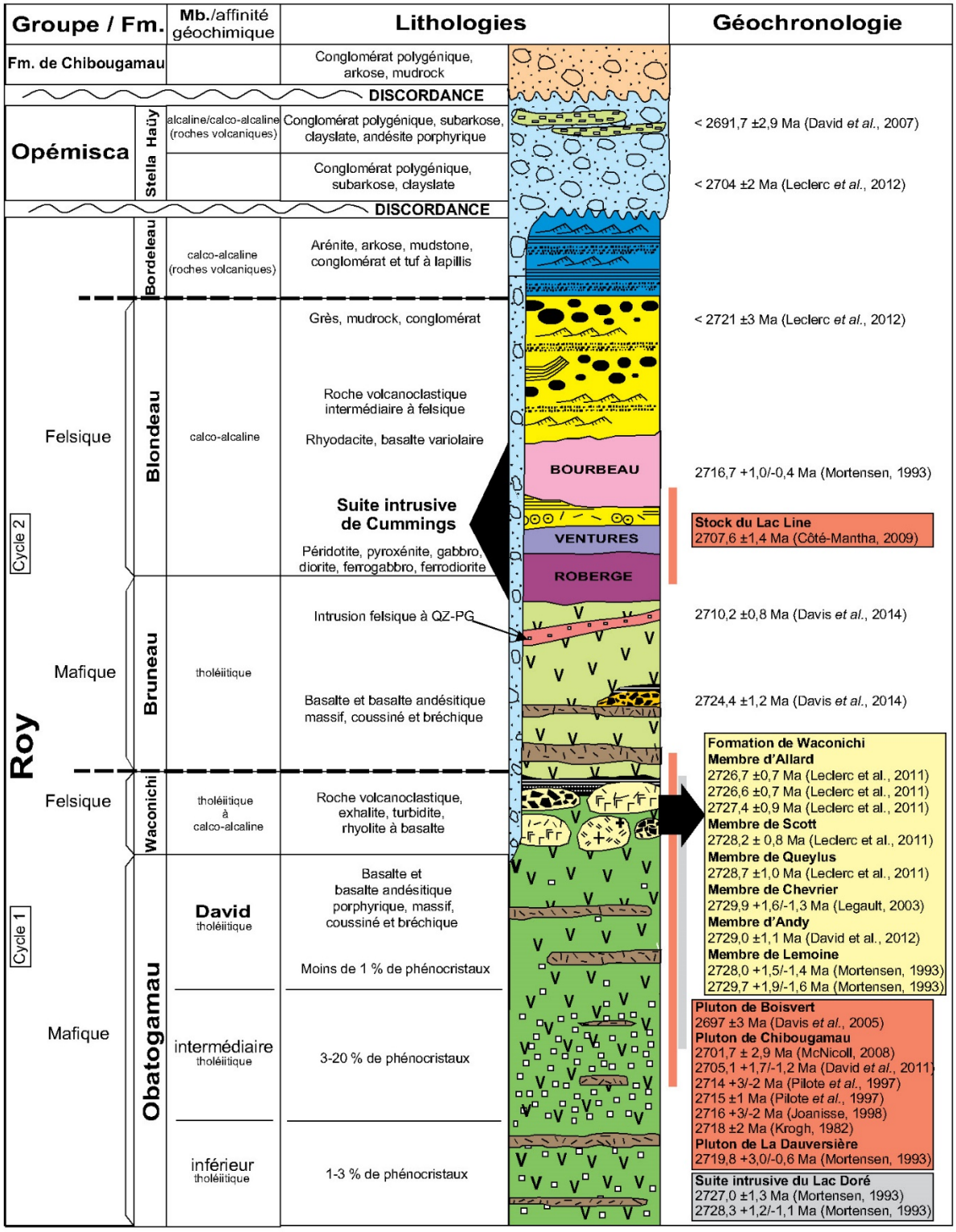

Figure 1-4. Stratigraphic relationships in the Chibougamau area (Leclerc et al. 2008,2011)

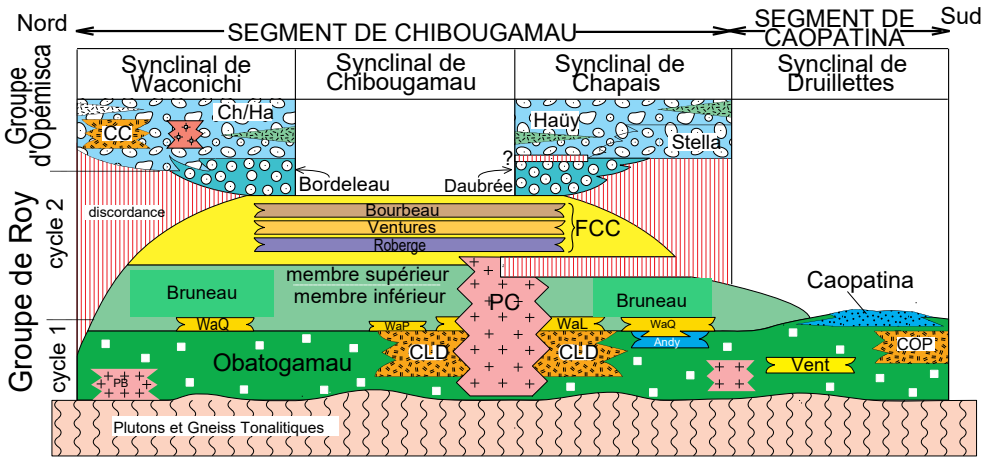

Figure 1-5. Generalized tectonostratigraphic relationships with respect to the position in synclines. See Figure 1-1 for abbreviations. Based on Gobeil and Racicot (1983) and Dimorth et al. (1984).

1.4 Research Questions to be Addressed by this Study

The question is can we modify the existing geological sections of the Chibougamau transect in a manner that is consistent with the surface geology and any drill holes and the petrophysical and geophysical data (gravity, magnetic and seismic). If we can build this section, does it tell us anything about the crustal structures and how they extent to the Earth's mantle? Can incorporation of multidisciplinary geological and geophysical information improve the reliability of the subsurface model? Do these structures represent a potential conduit of metals to endow mineral deposits in critical areas of the traverses?

The anticipated outcomes are sections showing the density, magnetic susceptibility variations as a function of depth, with any structures that are inferred from the data. The sections should be

consistent with the physical properties measurements, the geophysical data, and the known geology.

1.5 Structure of the remainder of the thesis

Chapter 2 starts with a brief review of gravity data acquisition during summer field 2017. The next section discusses gravity data processing, and different corrections to calculate the complete Bouguer anomaly.

Chapter 3 starts with the airborne magnetic data transformations, specifically applying some traditional directional and normalized derivatives to enhance the magnetic image. Information extraction from multiple derivatives was used to interpret surface geological features and boundaries associated with different magnetic properties. The next section presents the qualitative interpretation of the gravity data acquired by the Metal Earth project and the available GSC gravity data. This requires a consideration of the different constraints used in the potential-field forward modelling, such as (i) the results of qualitative interpretation of available airborne magnetic data, (ii) the surface geology and geological cross sections from previous studies, (iii) the interpretation of the Metal Earth seismic data, and (iv) the physical properties. The seismic data considered includes the historic Lithoprobe seismic data and the more recent ME seismic section.

Chapter 3 presents four forward modelled constrained geological cross sections from gravity and magnetic data, and their interpretations.

CHAPTER 2

2 Gravity data acquisition and processing

2.1 Introduction

To date, the Metal Earth project has acquired a total of 2974 gravity readings with an average spacing of 300 m along ~822 line kilometers spread across 10 transects. The first three transects were acquired during the data acquisition phase from 23rd of June to 25th of August 2017, namely Rouyn-Noranda (~93line km), Amos-Malartic (~88 line km), and Chibougamau. In this thesis, I focus on the data acquired along the Chibougamau transect (570 gravity observation along ~128 line kilometers oriented SW-NE). The Chibougamau gravity transect is coincident with the seismic transect and different from the A1-A5 and C1-C5 transects discussed above. Gravity data acquisition includes data collection, QA/QC and initial field processing. In conjunction, magnetic susceptibility measurements were made and rock samples for density measurements were collected from outcrops along the transects.

2.2 Gravity data acquisition

The gravity data was collected along exactly the same traverses as the seismic data were acquired. The stations were mostly chosen alongside roads or within walking distance of roads. The average spacing between observations is ~300 m, and according to sampling theory, this will allow anomalies greater that 600 m to be identified and perhaps modelled. However, where the profiles show discontinuities in slope, with sharp changes, an infill station was placed midway between the initial stations to more precisely define the subsurface structures (location, dip, and depth) more accurately. Also, in order to have data on small traverses perpendicular to the main

transect, three side road measurements with 300 m station spacing, for a total side traverse length of 900 m total, were acquired when side road access allowed.

Gravity data collected along a traverse is difficult to fit with two and a half dimensional (2.5D) models to greater accuracy than 0.5 milligals, so we are aiming for measurement precision of about 0.1 milligals. The largest changes in gravity are as a consequence of height changes, accounted for by the free-air and Bouguer corrections, which can be combined assuming a density of 2.67 g/cm^3 (Telford et al., 1990, equation 2.25) to give a gravity change of about 0.2 milligals per meter. Hence, the height of the station must be known to better than half a metre to achieve this precision. In the 2017 field season, we measured the height using a Juniper GPS system alongside the gravity meter. The GPS acquisition and differential post-processing is described in more detail below. Repeat measurements showed that the height accuracies were generally less than 30 cm, but occasionally of the order of a meter.

Magnetic susceptibility and samples for density measurements were collected when an outcrop was within 60 m of a gravity measurement. The coordinates of this data were only needed to this accuracy because the aeromagnetic data collected at a flying height of about 100 m is sensitive to an area that spans approximately 200 m, and this one location is taken as being representative of this larger area (Reid 1980). In this case, the team collecting the data would split up. One member would tend to the gravity data collection while the other would collect a rock sample and acquire magnetic-susceptibility measurements on the outcrop.

To collect magnetic susceptibility, a preferably fresh and flat surface with at least the same area as the KT-10 sensor (a circular area approximately 6 cm in diameter) is required. Once this is found, a reading can be taken, starting with a free air calibration by pressing the record button.

Where possible, the crew looked for locations that were the least weathered. This reading process was repeated a total of 10 times at different location on each outcrop. If there is more than one lithology, then ten readings for each different lithology. These 10 readings were taken to represent the rock materials and any geologic features running through them (Muir 2013). All the measurements were stored in a database for calculating central measures (mean or median) at each outcrop.

All gravity readings were taken using two geophysics crews equipped with two Scintrex CG-6 gravity meter instruments. For the traverse, two new gravity control points were established on the first day. These were tied to station 9003-1961 of the Canadian gravity standardization network (CGSN). The specifications of this station is shown in Figure 2-1, as well as a picture of one of our gravity readings at the station. An accurate reading of the gravity difference between the CGSN and the new control points was obtained by looping back and forth between the control point and the CGSN and taking at least five measurements (Kearey et al. 2012).

During data acquisition, readings were taken at control points at the start and end of each day. Each of these base station or control point readings comprise 600 raw gravity readings averaged over a 60 second measurement period, and the readings were repeated at least five times for every occupation. At all other stations, gravity was measured for 30 seconds and these readings were also repeated at least five times for each station and the average measured values were recorded for the station (Yushkin 2011; Scintrex 2018).

In order to compare the measurements from the two CG-6 instruments with each other, ten percent of the total number of measurements were selected to be measured by both instruments. Also, in order to evaluate the accuracy of the data measured by each device during the day, one

station was selected for each crew to be measured at the beginning, middle, and at the end of each day.

Gravity (CGSN)

Download Report

Site Identification				
Name	**Province**	**Unique Number**	**Description**	**Last Inspection**
CHIBOUGAMAU	QC	9003-1961	LAC CACHE FECTEAU	09/1976

Station Coordinates (Scaled)					
Latitude	**Longitude**	**Elevation**	**Gravity Value**	**HI**	**Gradient**
N49° 49' 25" ± 20.0 m	W74° 25' 33" ± 20.0 m	375.00 ± 3.00 m	980925.2300 ± .0240 mGal	0.15 m	0.3086 mGal/m

Station Description

The station is located at Fecteau Transport Seaplane Base; on concrete base of the southernmost antenna mast, immediately NE of office building. Station is monumented with aluminum disc.

Stations with same name

No other stations with the same name

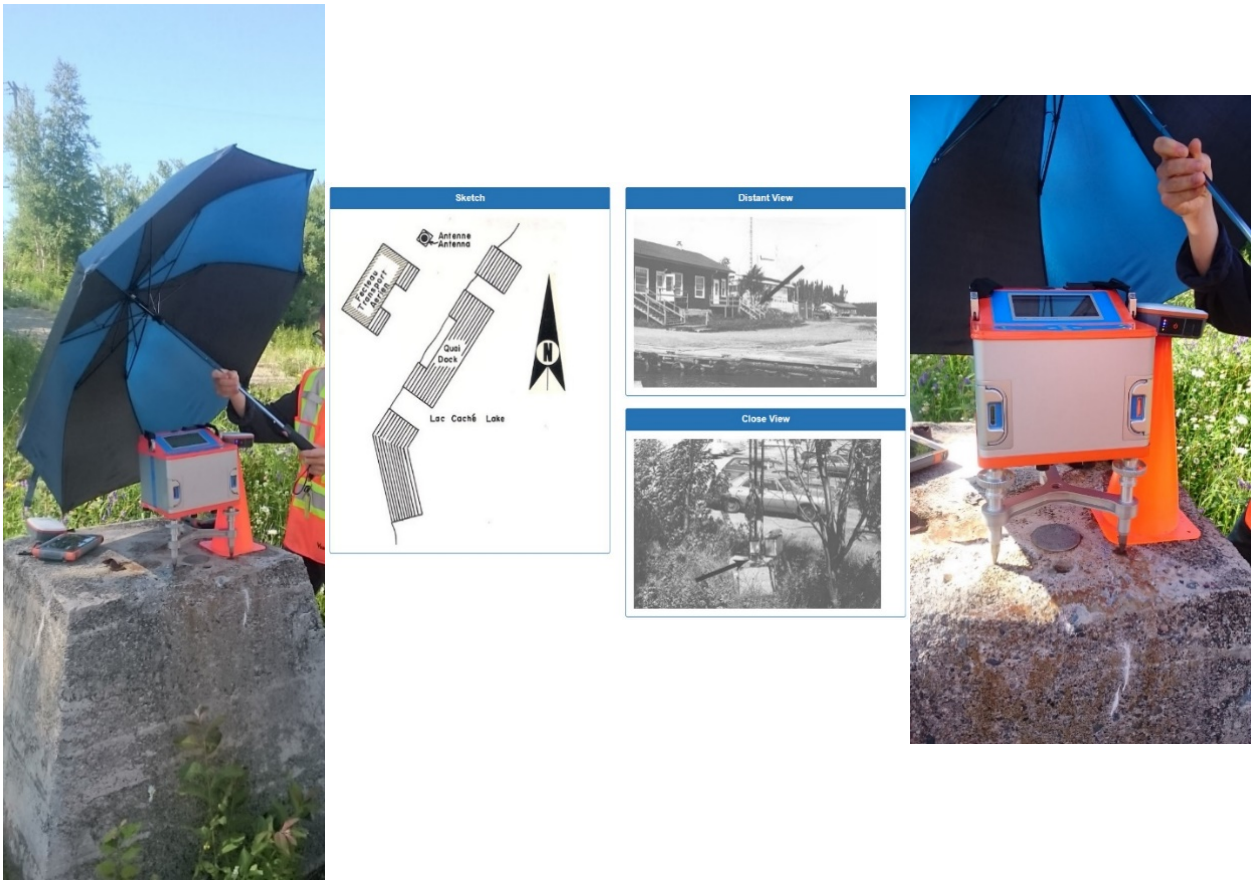

Figure 2-1. (top) Specifications for the Chibougamau base station, a member of the Canadian gravity standardization network(CGSN). (bottom) acquiring gravity data at this site.

Global Navigation Satellite System (GNSS) data (GPS, GLONASS, etc.) were acquired using a Juniper Systems Geode handheld device. Data from each unit was downloaded to a laptop every evening, along with data from a nearby government GPS base station, which was processed using EZSurv post-processing differential correction software. The output from this software was an ASCII file containing station numbers, eastings, northings, heights, and the respective errors. The final data is stored in the Geographic Coordinate System (Datum) of NAD83 – Canadian Spatial Reference System (Zone 18N). This Geode system required about 8 minutes for acquisition at each station to get readings at the required accuracy, with some stations barely being accurate enough. Figure 2-2 shows the acquired gravity stations, control points, and Chibougamau base station location along the Chibougamau transect.

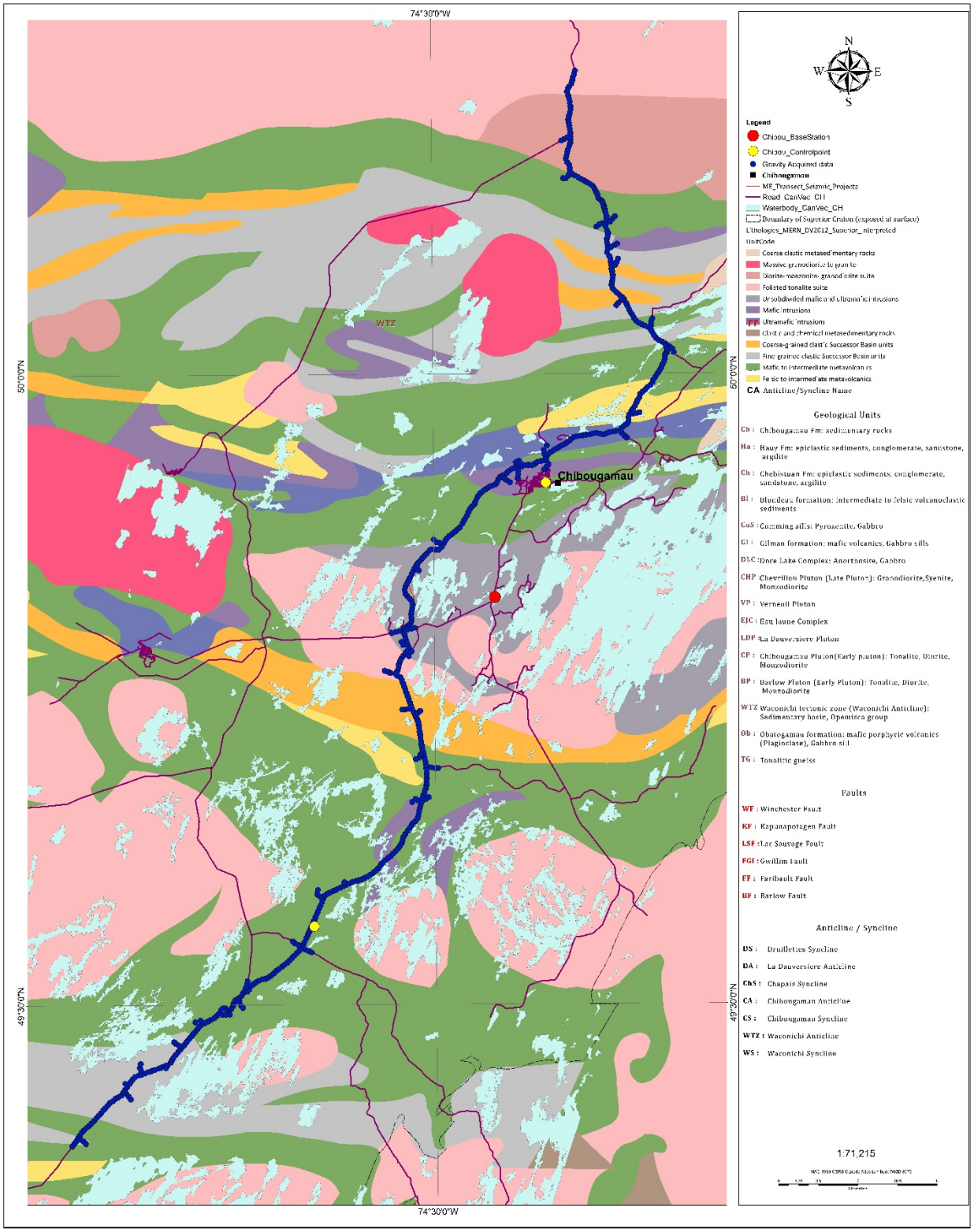

Figure 2-2. The acquired gravity data (blue), control points (yellow), and Chibougamau base station (red) along the Chibougamau transect. Modified after (Montsion et al. 2017).

2.3 Gravity data processing

The first step in field processing of the gravity data was to check for drift errors. Drift has been defined as the difference between the readings at the base stations at the start and end of the day. These drifts were interpolated to the time that data was acquired at each station and used to correct for the drift of the instrument at that station.

The positional data from the differential GPS processing was then associated with each gravity reading. Therefore, each record consisted of station number, easting, northing, orthometric height and difference from the gravity at the base station.

The CG6 gravity meter uses the position and time from an internal GPS system to calculate an earth-tide correction. Subsequent field processing of the gravity data at each station involved the following (Kearey et al. 2012):

- Calculate the observed gravity (G_{obs}) (mGal).

  $$G_{obs} = G_{base} + difference\ from\ base$$

- Calculate the theoretical gravity (G_{the}) (mGal). Geological Survey of Canada (GSC) has used the 1967 International Gravity Formula as given below, and using this formula rather than some other formula allows us to have consistent datasets with GSC gravity observations.

  $$G_{the} = 978031.846(1 + 0.005278895sin^2\lambda + 0.000023462sin^4\lambda)$$

  where λ is the latitude of the station in radians.

- Calculate the free-air correction (FA) (mGal). This corrects for the height of the station above the geoid and is equal to a reduction of 0.3086 mGal per metre. In this equation, h is the station's height above the geoid in metres.

$$FA = -0.3086h$$

- Calculate the Bouguer correction (BC) (mGal). This corrects for the mass between the station and the ellipsoid/geoid. In this equation, ρ is the density of rocks between the station and the geoid. The value of 2.67 g/cm^3 was adopted as it is representative of our area.

$$BC = 0.04191\rho h$$

- Calculate the terrain correction (TC) (mGal). The Bouguer correction assumed a flat topography around each gravity station, so the terrain correction (TC) accounts for topographic relief in the vicinity of the gravity station (Kearey et al. 2012). I used the Geosoft Oasis montaj software (Geosoft, 2015) to calculate this correction, which comprised multiple parts. The corrections for topographic variations more than local correction distance, 3000 m, from the station are calculated using the "Create Regional Correction Grid" dialog in Geosoft. This regional correction uses a coarse regional Digital Elevation Model (DEM) with a 250m cell size. The correction applies to an area up to 167 km beyond the station (Nowell 1999), so this step is computationally expensive. The "Terrain Correction" tool is used for the terrain correction, which uses a more finely sampled local DEM grid, with a 30m cell size, that covers the survey area. These corrections all assume a flat earth. The final Bullard B correction accounts for the curvature of the Earth which has an impact beyond a radius of 167 km from the station location (Nowell 1999). The default value 2.67 g/cm^3 was used for the terrain density.
- Finally, calculate the complete Bouguer Anomaly (CBA) (mGal) using the formula

$$CBA = G_{obs} - FA - BC + TC - G_{theo}$$

Figure 2-3 illustrates elevation, free air anomaly, and complete Bouguer anomaly for each station along the Chibougamau transect.

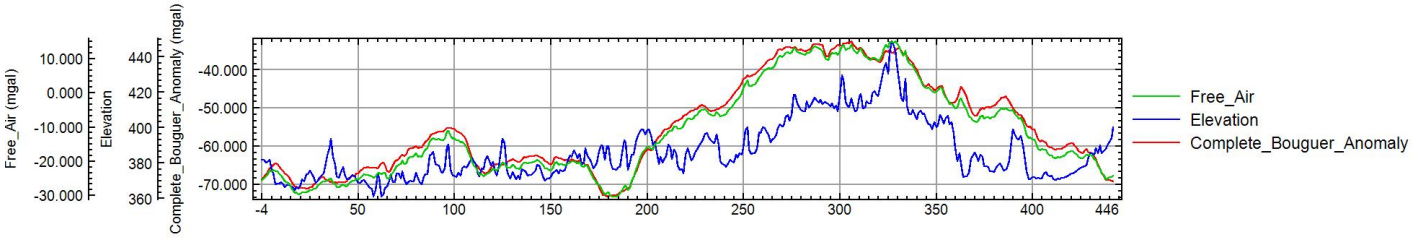

Figure 2-3 The elevation, free air anomaly, and complete Bouguer anomaly for each station along the Chibougamau transect.

Chapter 3

3 Constrained potential field data modelling and interpretation

3.1 Introduction

The question in this chapter is whether it is possible to build a petrophysical section of the Chibougamau transect that is consistent with the known geology and the petrophysical and geophysical data and what does it tell us about the crustal structures? The significance of these crustal structures on the metallogeny will become clearer when geochemical, alteration and other data is included at later stages of the Metal Earth project. The anticipated outcomes are sections showing the density, magnetic susceptibility variations as a function of depth, with any structures that are inferred from the data.

In this research, the potential-field data along the Chibougamau transect located in the northeastern part of the Abitibi sub-province is considered. The gravity data collected for the Metal Earth project along the transect was merged with the available data from the Geological Survey of Canada (GSC).

The magnetic data was microlevelled aeromagnetic grid with a spatial resolution (grid cell size) of 75 m generated from existing magnetic grids from the Ministère de l'Énergie et Ressources Naturelles du Québec (MERN). Geosoft Oasis Montaj was used to enhance the images and highlight the edges of magnetized bodies and near-surface lineaments.

The seismic data from the ME project were processed using the procedures of Naghizadeh et al. (2019), in particular, the curvelet enhanced data were used to interpret the regional (R1) seismic

data from the ME in order to reveal reflections, that can be used as a constraint in potential field-data forward modelling.

Gravity and compiled high-resolution magnetic data along this transect were modelled using an initial petrophysical model constrained by geological observations made at the surface, seismic sections at depth and measured petrophysical properties. The Geosoft GMSYS software was used to do this forward modelling of gravity and magnetic data. For the modelling, the crooked Chibougamau transect had to be broken into four straight profiles. This modelling will provide information about the distribution of magnetic subsurface material and the density of rocks, and structural details especially in areas where the seismic data shows no strong reflections. Previous seismic data indicate that Moho depths in the Abitibi greenstone belt do not exceed 40 km (Ludden, 2000; Calvert and Ludden, 1999), which is consistent with Winardhi and Mereu (1997) and Mereu (2000) who interpreted refraction data to determine a Moho depths of 37–40 km in the Abitibi subprovince. Hence the Moho depth was considered 35-36 km in the potential-field modelling. Also, the lower crust depth was set to 26 km and its density was set to 2.95 g/cm^3 while the upper mantle was set to 3.3 g/cm^3 (Telmat et al., 2000).

3.2 Geophysical setting

Geological features such as the synclinorium and anticlinorium of volcanic and sedimentary in the Chibougamau area, and other features of interest such as plutonic intrusions, and structures can be mapped in detail from the gravity and magnetic data as discussed in the next sections.

3.2.1 Qualitative interpretation of the airborne magnetic data of the Chibougamau area of interest

3.2.1.1 Introduction

Magnetic field data are fundamental to geophysical approaches for geological mapping. Airborne total magnetic intensity data (TMI) over the Chibougamau area of interest were used to generated some traditional directional and normalized derivative images in order to (i) delineate boundaries associated with different magnetic properties (e.g., faults, and lineaments), (ii) identify folds, (iii) intrusions, and (iv) outline possible metamorphic zones associated with the creation or destruction of magnetic minerals. These images were interpreted on screen on a GIS system to locate lateral changes in the magnetization of the outcrops and extend these into sparsely exposed or completely covered areas.

3.2.1.2 Magnetic data transformation and enhancement

The aeromagnetic grids were reduced to the pole and vertical derivatives, tilt angle, analytic signals were applied to enhance the edges of magnetized bodies and near-surface lineaments.

The magnetic method primarily maps the spatial distribution of ferromagnetic material such as magnetite and pyrrhotite, but it can also map heterogeneities associated with alteration and metamorphism (Olaniyan et al., 2013 and Dentith and Mudge, 2014). Therefore, it is important to have an appropriate geology knowledge of the study area during processing and interpreting of a magnetic dataset.

Figure 3-1 shows the total-magnetic-intensity field (TMI) of the Chibougamau area of interest. To the north of the Chibougamau pluton, mafic to intermediate metavolcanics of the Gilman formation, and mafic/ultramafic intrusions of the Cummings sills have the strongest magnetic intensity. The granodioritic to granitic plutons such as the Chibougamau pluton exhibit weak magnetic intensity, while intermediate metavolcanics and sedimentary rocks have weak to moderately high magnetic intensity. Most magnetic lineaments (presumably dykes) with SW-NE and SE-NW direction have high magnetic intensity.

The magnetic images comprise of a wide range of short- and long-wavelength information related to shallow and deeper sources (Spector and Grant 1970), each with different geometry, depth, and size. So a combination of contact mapping methods has been developed to delineate the magnetic contact and lineaments (Pilkington and Keating 2010). In this work, I have computed traditional directional and normalized derivatives such as the tilt derivative (Miller and Singh, 1994), the total horizontal derivative (TDX) (Cooper and Cowan, 2006), the vertical derivative (Hood, 1965) from reduced to pole data to delineate surface geological features, and boundaries associated with different magnetic properties, lineaments (e.g., faults, folds), intrusions, and for outlining possible metamorphic zones associated with the creation or destruction of magnetic minerals (Olaniyan et al. 2013). The directional derivative of the TMI highlights the shorter wavelength portion that corresponds to the near-surface geological structure, and was used to calculate the tilt derivative and TDX derivative in order to enhance subtle anomalies and show anomalies over magnetic anomalies.

For the Chibougamau data set, I found that a combination of the vertical derivative image in colour and the tilt angle image in gray scale (Figure 3-2) delineates linear discontinuities and structural patterns, such as faults and dykes, and different rock units. The discontinuities with

low magnetic contrast are generally associated with major faults drawn on the geological maps, and the SE-NW, SW-NE trending mafic dykes show a strong magnetic contrast relative to their host rock. The filtered tilt angle derivative map (Figure 3-3), restricted to show only values greater than 0, illustrates mostly SE-NW and SW-NE trending dykes with strong magnetic anomalies.

3.2.1.3 Magnetic interpretation map

My approach in digitizing and polygonising the contact of two magnetic units was primarily to draw a contact where there was a change in the magnetic fabric between the units, as this reflects differences in the magnetic texture (Olaniyan et al. 2013). These textural changes may reflect differences in the magnetic mineral content of rocks and potential changes in grain shapes and preferred crystallographic orientation of magnetic minerals (Hrouda and Kapička 1986). The digitized linear information was categorized as dyke, fault, and lithological contact if there was a close association with known features on the geological map. Otherwise, they were labeled as other lineaments (Figure 3-4).

In order to assess the quality of the geophysical interpretation in Figure 3-4, the geological boundaries were overlain on interpreted magnetic contacts and lineaments. Generally, the defined lithological boundaries are mostly consistent with the interpreted magnetic contacts, but, in some cases because of varying degrees of magnetic mineral alteration in the rocks close to contacts, or inaccessibility issues as a consequence of swamps and lakes, there is a good argument for adjusting the geological boundary. The magnetic interpretation map (Figure 3-4) also shows a magnetic stratigraphic map and magnetic lineaments.

The magnetic interpretation results were used as surficial geological constraints in the 2.5-D potential-field data modelling because the SE-NW, SW-NE trending dykes were only partly mapped on the large-scale geological map and it was necessary to know where they crossed the traverse in order to model the magnetic data.

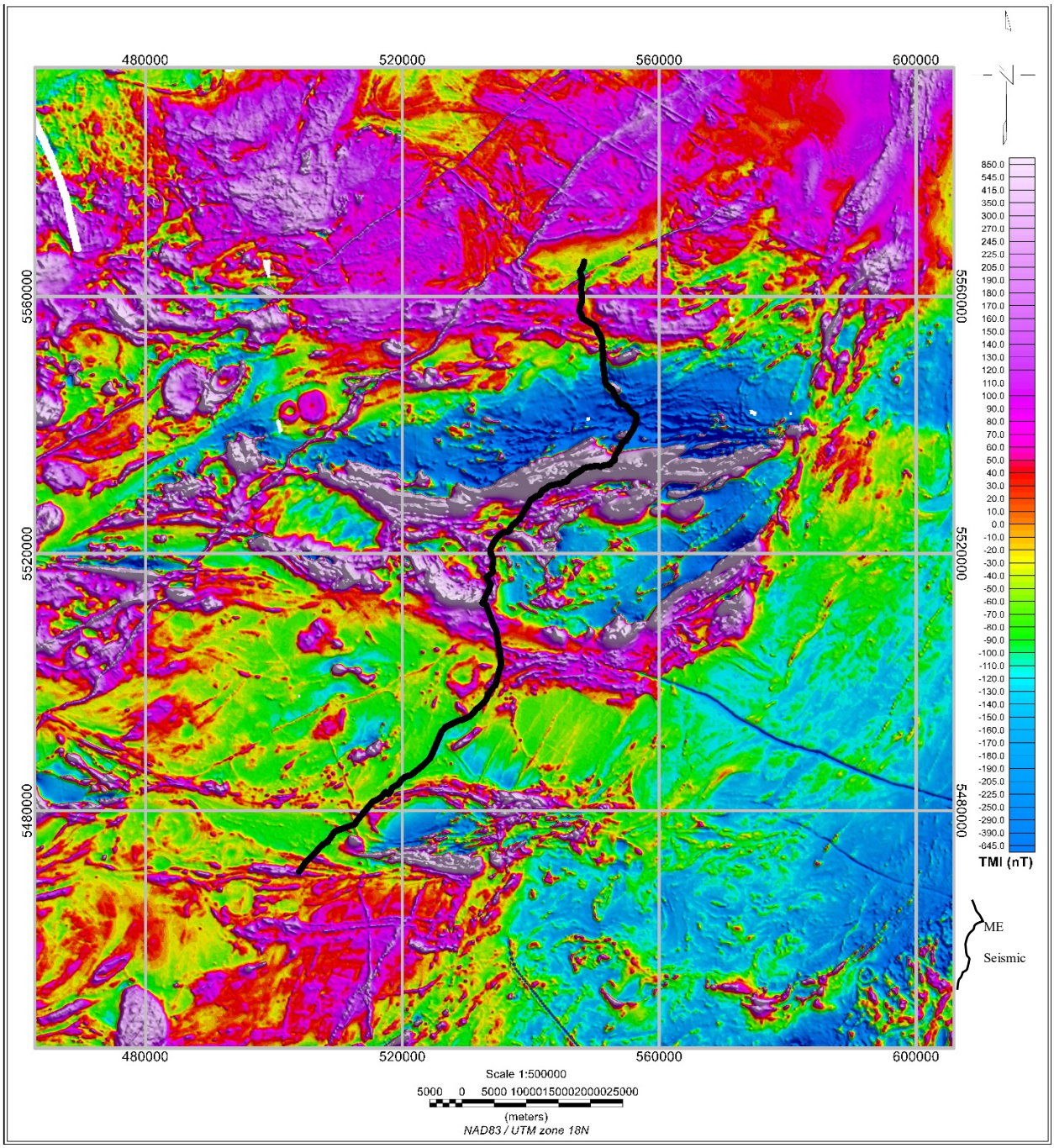

Figure 3-1. Total magnetic intensity of Chibougamau area of interest.

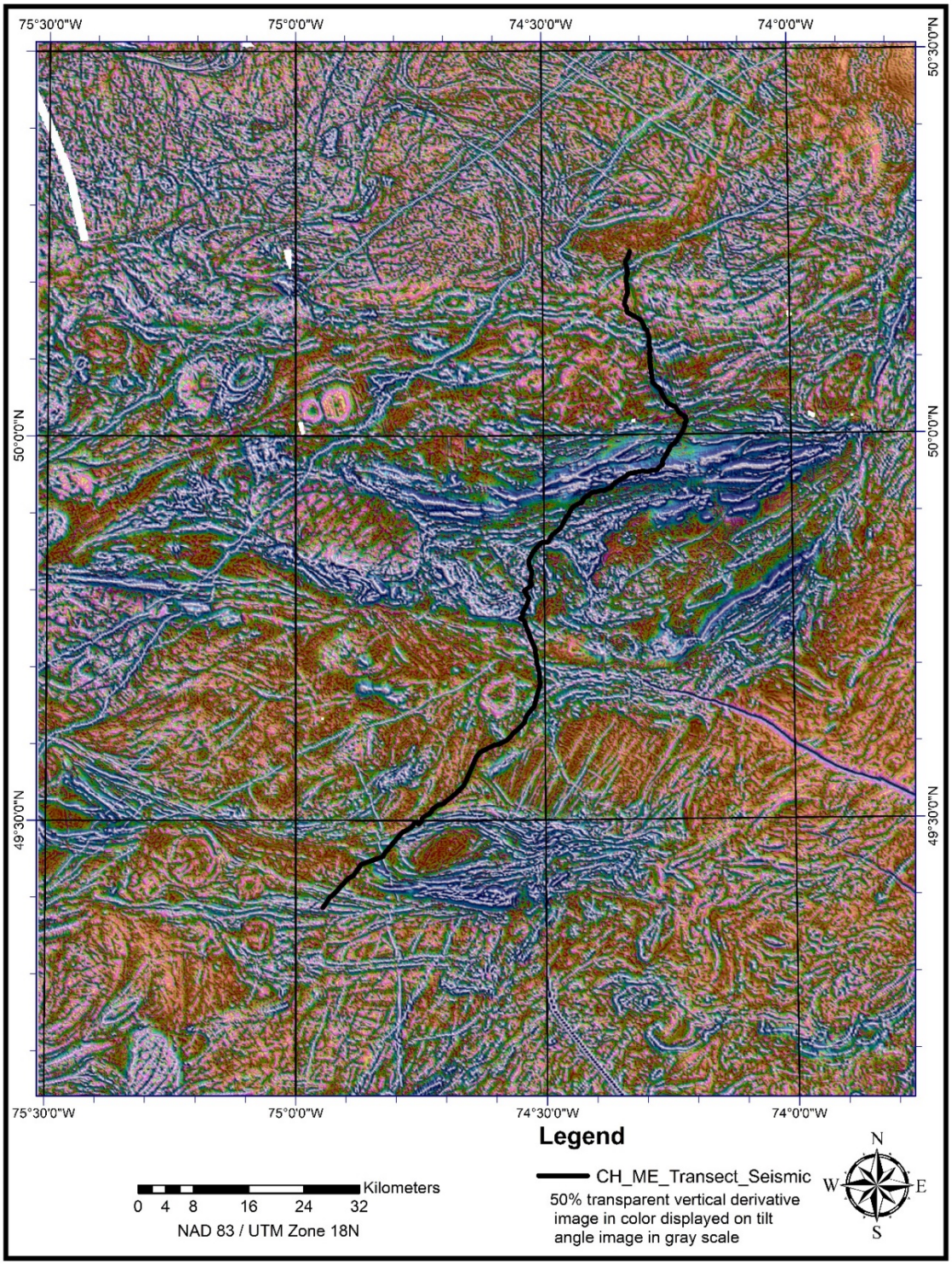

Figure 3-2. Combination of 2nd vertical derivative and tilt angle images of the Chibougamau area of interest. There is no color bar, as this image is intended for qualitative interpretation of structures.

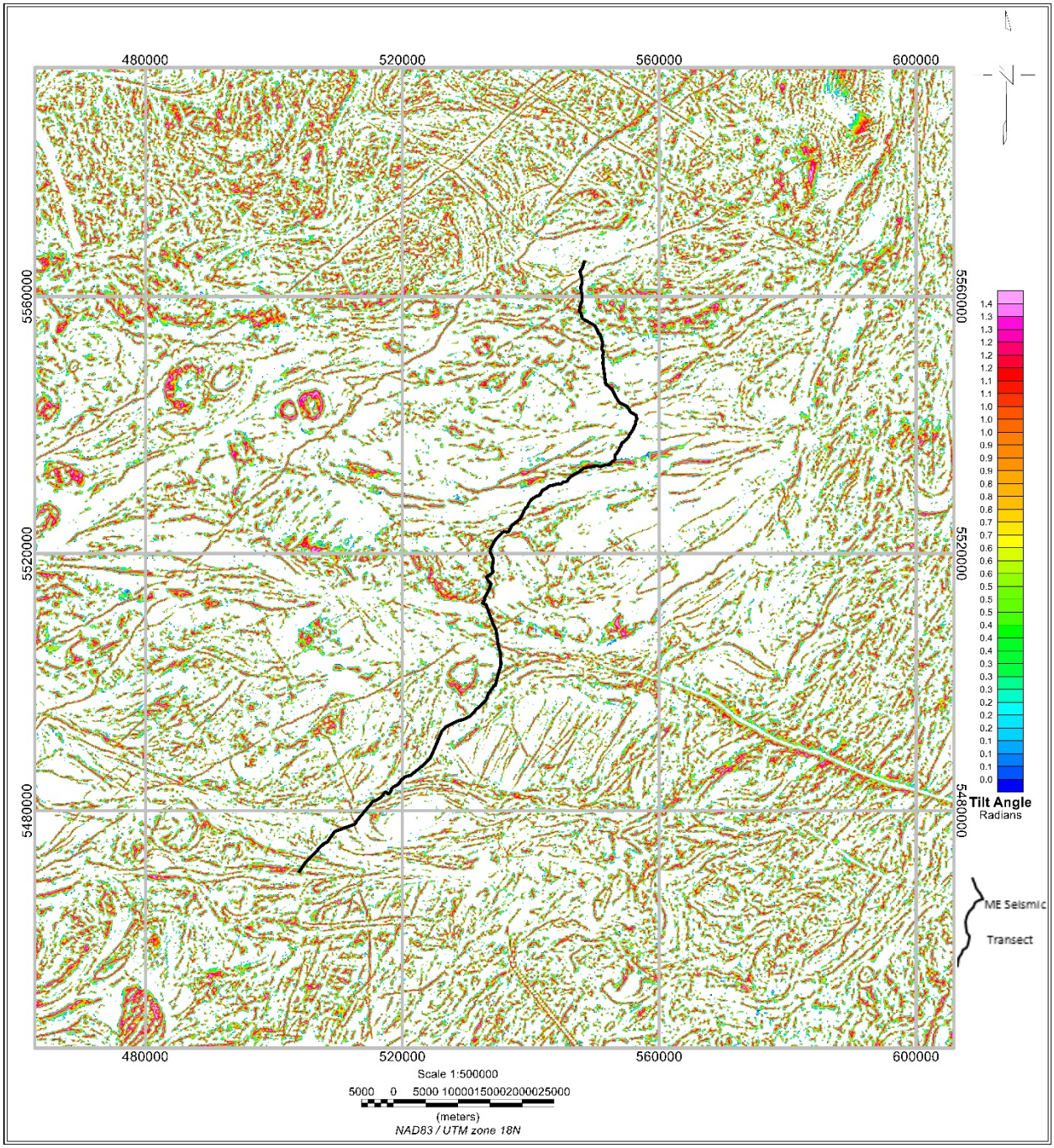

Figure 3-3. Filtered tilt-angle derivative of the TMI, with values less than zero shown as white.

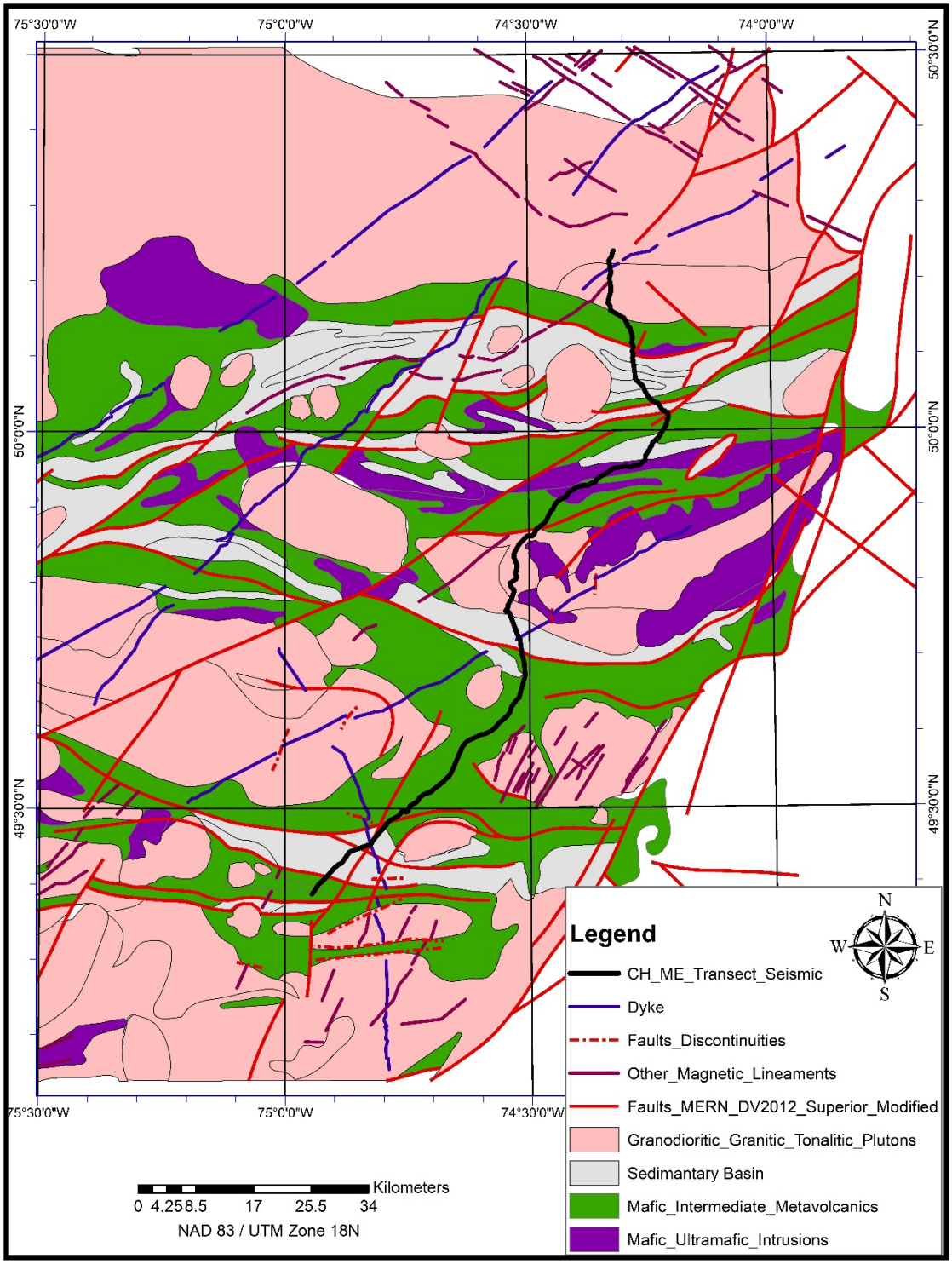

Figure 3-4. The magnetic interpretation map showing magnetic stratigraphy, lineaments and dykes.

3.2.2 Qualitative interpretation of the gravity data of the Chibougamau area of interest

The first step in combining the Metal Earth gravity data along the transect with the available data from the Geological Survey of Canada (GSC), was to assess the quality of the GSC data. Because the main source of error in gravity data is a consequence of elevation error (Telmat et al. 2000), I looked at the height uncertainties and found there were two different categories of data. In the first group, collected before 1964 with barometric altimeters the elevation uncertainty was more than 1 meter. In the second group, the elevation was determined with an accuracy of less than 1 meter. So the first group of GSC data was deleted from the data set and the remaining data was processed using Geosoft Oasis Montaj to calculate complete Bouguer anomaly and combined with the ME data (Figure 3-5).

The Bouguer anomaly (Figure 3-5) ranges from -87 to -34 mGal. The lowest values are associated with the Chibougamau and Opemisca plutons, which correspond to tonalitic, granodioritic, granitic plutons with an average density of 2.67 g/cm^3 and 2,63 g/cm^3. Getting closer to the heart of the Chibougamau pluton, the values fall quickly which could be due to the increasing thickness of the pluton. Mafic-ultramafic intrusions and volcanic bands locate to the north of the Chibougamau pluton and to the south and north-east of the Opemisca pluton show elongated zones with highest values of the Bouguer anomaly.

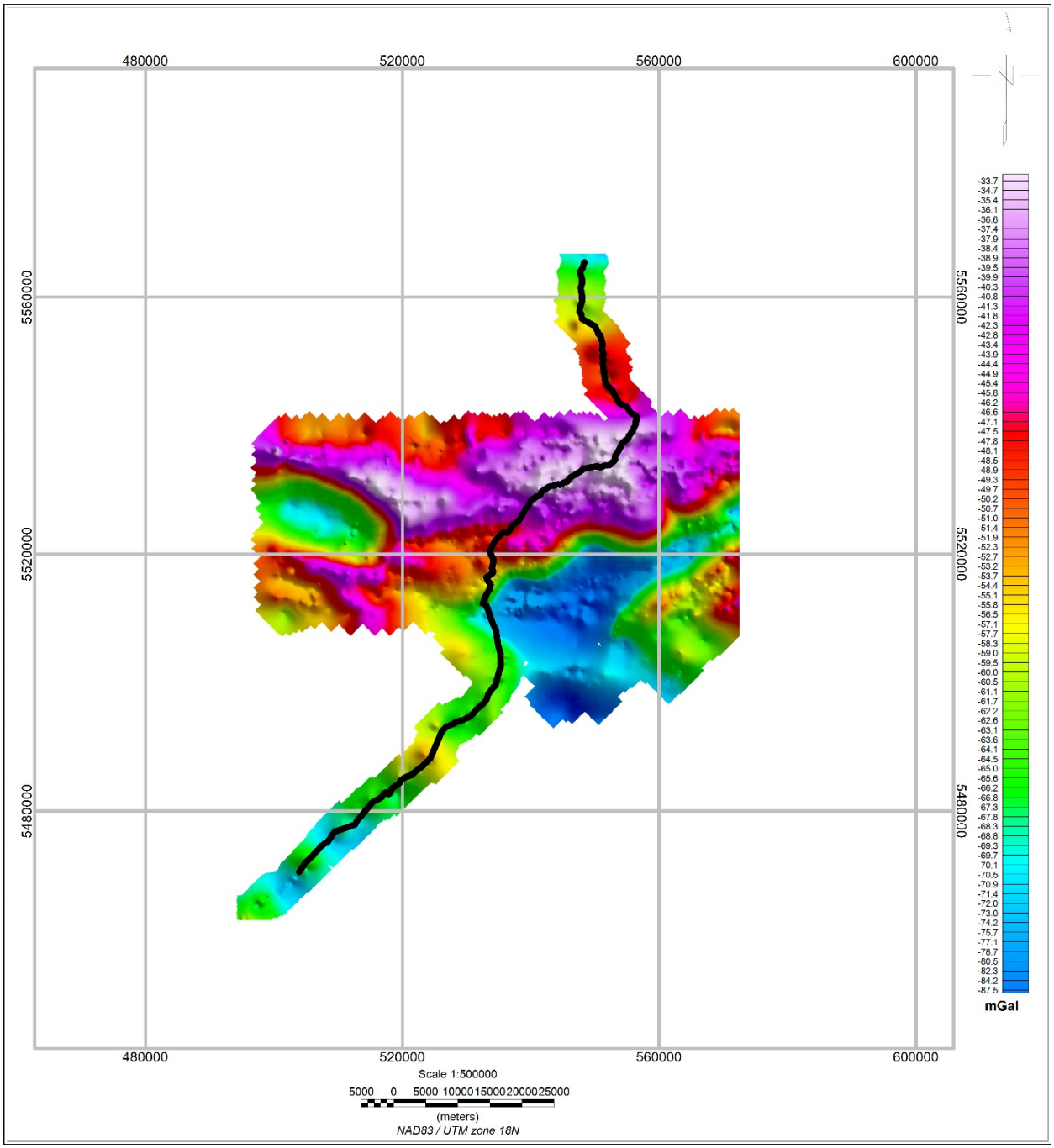

Figure 3-5. Complete Bouguer anomaly map of combined ME and GSC gravity data. The ME stations are shown with black dots on the map. The GSC stations cover the remaining area at ~1000 m station spacing.

3.3 Forward modelling of gravity and magnetic data

Geosoft GMSYS software was used to do forward modelling of gravity and magnetic data for four straight profiles along the crooked Chibougamau transect (Figure 3-6). The purpose of the modelling is to provide information about the distribution of magnetic subsurface material and the density of rocks, and structural details especially in areas where there is little information available from the seismic investigations. The complete Bouguer anomaly and total magnetic field were forward modelled by adjusting the shape and physical properties of different geological units in order to minimize the differences between the modelled and the observed data. Because the physical properties can vary within each geological unit based on alteration (Morris, 2006), metamorphism, and faulting, a single value is not appropriate for each rock type. Eshaghi et al. (2019) demonstrate that many lithologies show a statistical distribution and in many cases a multi-modal distribution of physical properties. Hence the physical properties can be assigned values within a range. Further, the magnetic susceptibility can be increased or decreased from its actual value to take into account normal or reversed remanent magnetization.

3.4 Constraints on the 2.5-D model

Because the non-uniqueness of potential field data means that different petrophysical models which can match the same observed geophysical data, it is necessary to apply surficial/sub surficial geometric and petrophysical constraints to make the model geologically reasonable. These constraints come from the following sources:

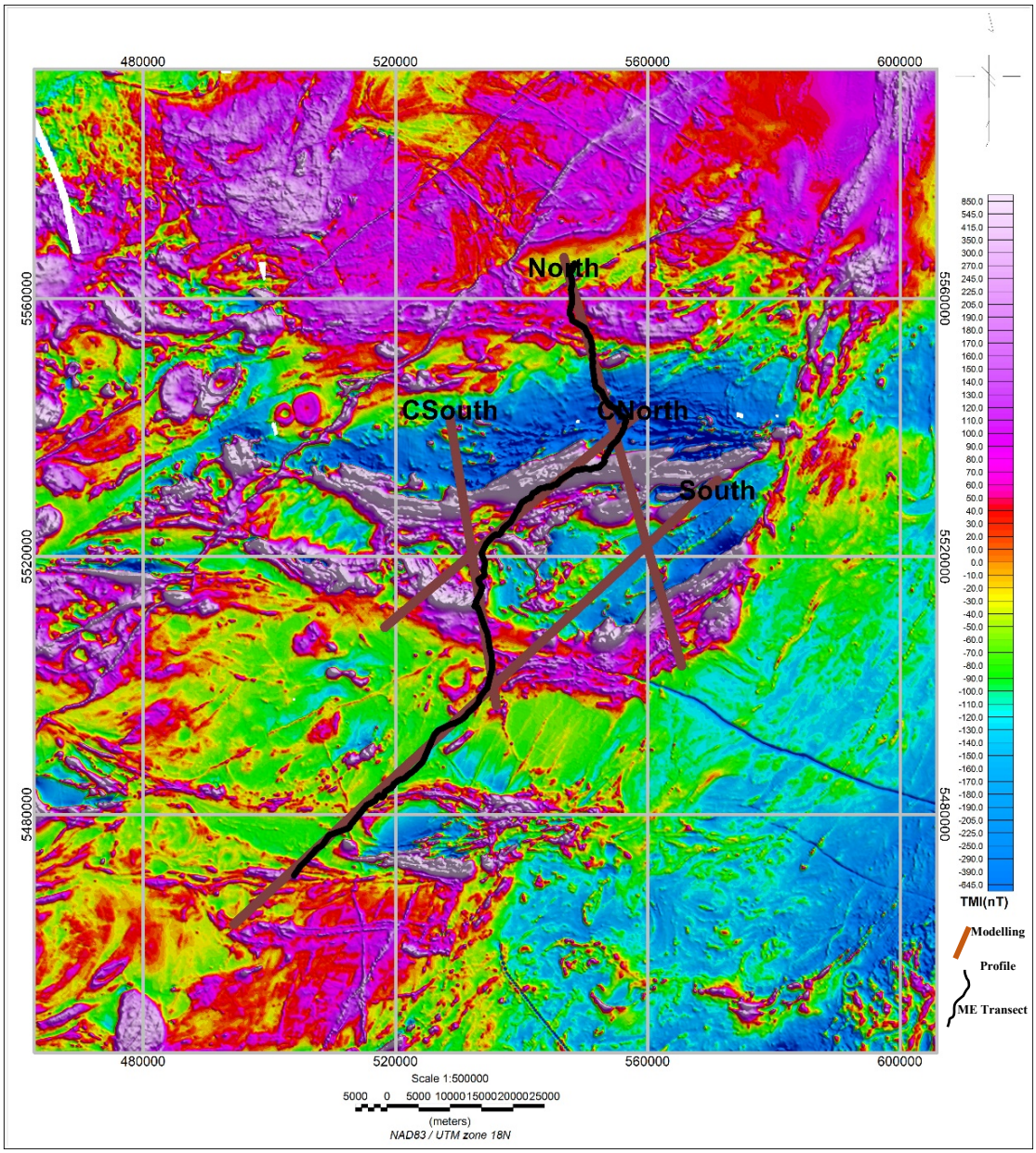

Figure 3-6. The location of the forward modelled sections on the TMI map. The black line is the Chibougamau transect and brown lines are the modelled profiles.

3.4.1 Magneto-stratigraphic map

The surface geological map (modified from Montsion et al. 2017, Daigneault et al. 1990, Leclerc et al. 2008) was used to constraint the geometry of the models in the surface. In some cases, this was adjusted if the magnetic interpretation indicated the geological map was not consistent with the magnetic data. Primarily, this meant adding some additional magnetic lineaments (dykes and faults), and some adjustments in the location of mapped geological contacts (Figure 3-4). Specifically, there are some N-S directed lineaments (dykes) added in the southern part of the "South" model and the location of the Dore Lac complex in the intersection of "CSouth" and "CNorth" models were adjusted.

3.4.2 Geological section

There were four published geological cross sections available from previous geological studies in the Chibougamau area (Figure 1-2), and from geophysical gravity forward modelling in the Chapais area (Figure 3-7). Drill-hole logs were not used as part of this study to extrapolate surface features into the sub-surface. If these logs could be found, it is unlikely that they would provide information at the depths of interest. I assumed that any structural and drill information was used when building the cross sections, so these were used as a guide when constructing the petrophysical model for forward modelling.

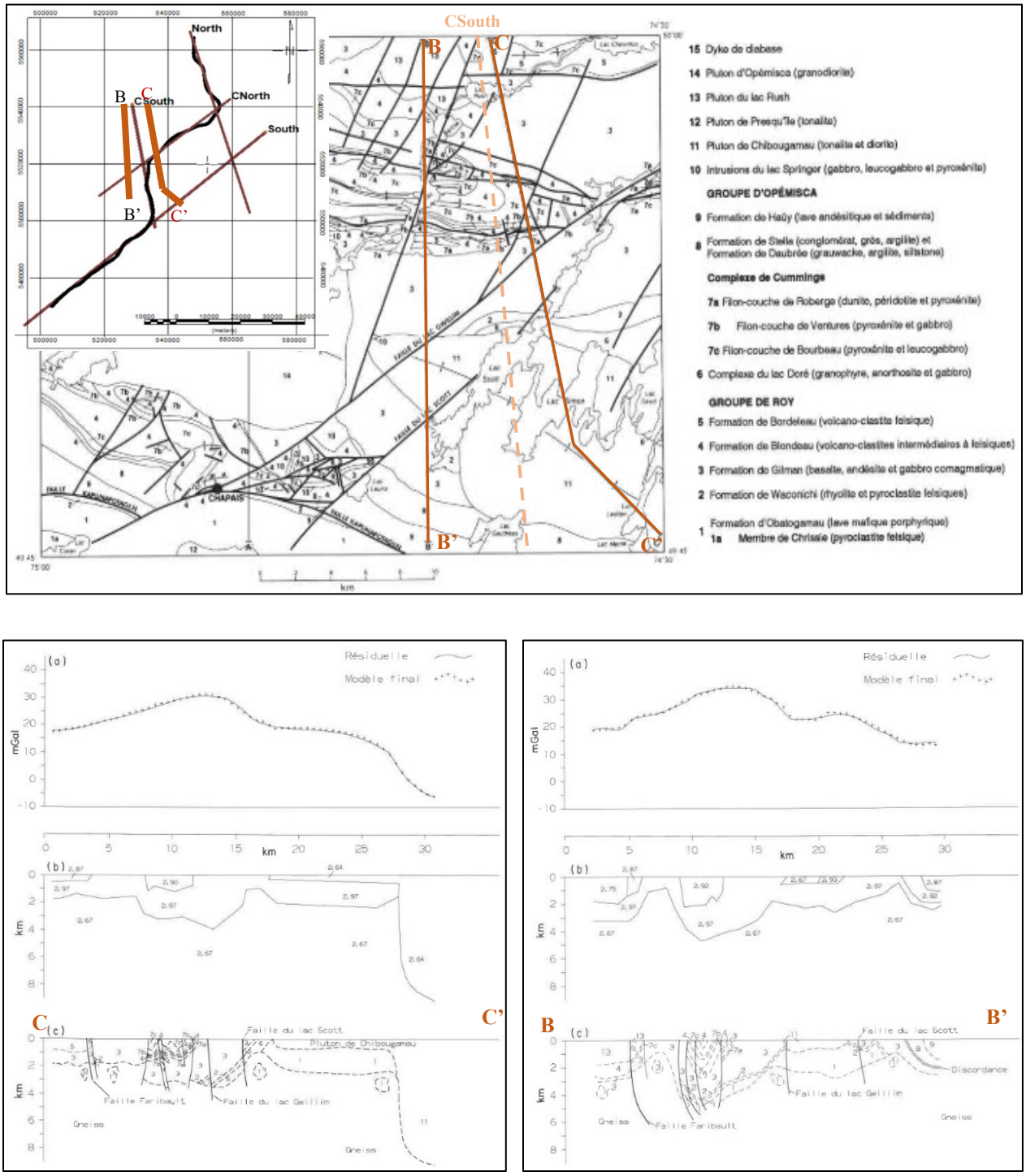

Figure 3-7. Geological sections from previous geophysical studies (Dion et al. 1992), Two brown solid lines BB' and CC' shows the location of two geological cross section modelled from geophysical gravity data in the Chapais area, and the dashed orange line illustrates the north part of the CSouth profile of this study.

3.4.3 Seismic sections

Between 1988 and 1993, the Lithoprobe program acquired three seismic reflection profiles across the eastern part of the Superior province. These profiles traversed (i) the Opatica plutonic belt, (ii) the Abitibi granite-greenstone belt, and (iii) the Pontiac metasedimentary sub-province (Figure 3-8). The purpose of these profiles was to define the geometry of the crustal structure at depth (Calvert and Ludden, 1999). Line 48 is the closest Lithoprobe line to Chibougamau's Metal Earth transect, which is located ~300 km in the west. Calvert and Ludden (1999) interpreted the reflector patterns and the combined litho-seismic section shows shallow north dipping reflections with northward under-thrusting or subduction zone in the upper mantle below the Opatica plutonic gneiss belt (Benn et at., 1992; Sawyer and Benn, 1993) (Figure 3-9). Calvert and Ludden (1999) interpreted the mid-crust Abitibi belt as being composed of metasedimentary and igneous rocks with some unknown affinity units, and the Opatica belt mainly comprises orthogneissic rocks. In a location west of these profiles, Mint (2017) believes that a fragment of the middle and lower crust in the Superior Province has been transported to the surface within the nearly north-south Kapuskasing reverse–thrust fault zone. This zone consists of mafic, tonalitic, and metasedimentary gneisses of amphibolite and granulite facies.

3.4.3.1 The Metal Earth's seismic survey

The Metal Earth project acquired 927 km of deep seismic reflection profiles from August to November of 2017 in the Abitibi and Wabigoon greenstone belts of the Superior craton. The intent of the seismic surveys was to image structures from the near-surface to Moho depths.

The Chibougamau seismic reflection profile is the easternmost of these profiles and was acquired entirely on gravel roads. The ME project collected data in a number of modes regional (R1) data,

high resolution (R2) data and long offset full-waveform data (R3). The specifications for these modes is shown in Table 3-1. For this study, only the regional (R1) data had been processed.

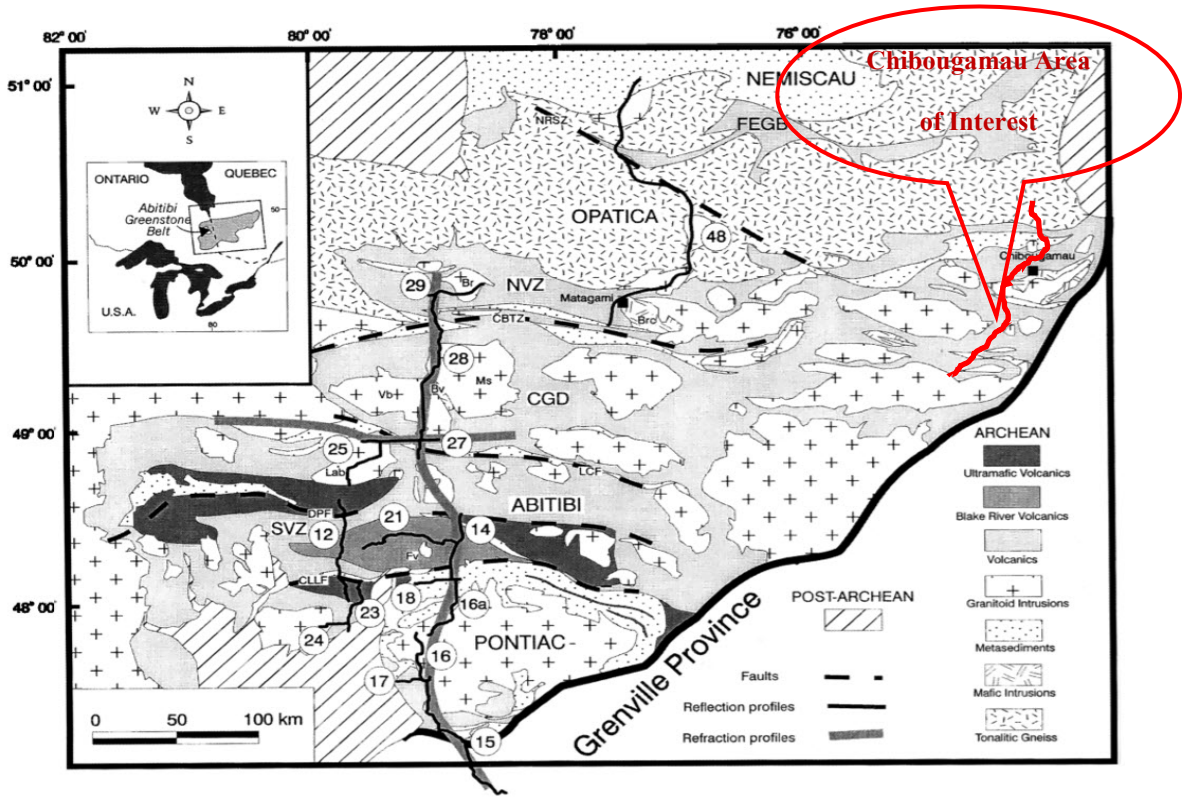

Figure 3-8. Generalized geological map of the southern Superior Province. The locations of the different seismic lines acquired as part of the Lithoprobe Abitibi program are indicated. The seismic reflection transects comprise three parts, separated by east-west offsets: line 48 across the Opatica plutonic belt, a group of lines (15 to 29) across the Pontiac metasedimentary belt and the Abitibi greenstone belt. FEGB, Frotet-Evans greenstone belt; NVZ, Northern Volcanic Zone; CGD, Central Granite-Gneiss Domain; SVZ, Southern Volcanic Zone; NRSZ, Nottaway River shear zone; CBTZ, Casa-Beradi tectonic zone; LCF, Lac Chicobi fault; DPF, Destor-Porcupine fault; CLLF, Cadillac-Larder Lake fault; Br, Brouillan pluton; BRC, Bel River Complex; Vb, Villebois pluton; Bv, Boivin intrusion; Ms, Mistouac pluton; Lab, Lac Abitibi pluton; FV, Flavrian pluton. Modified after (Calvert and Ludden, 1999). Red crooked line on right hand side shows the Chibougamau transect.

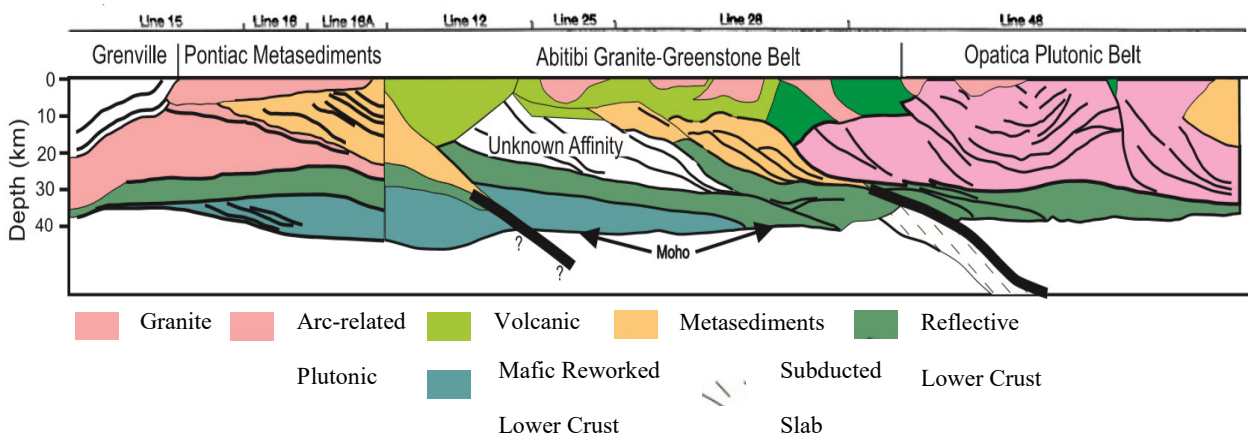

Figure 3-9. Interpretation of the projected North-South seismic sections along the Lithoprobe corridor shown in Figure 3-8. Modified after (Calvert and Ludden, 1999). The profile locations are already shown on 3-8.

Table 3-1. Acquisition parameters used in regional (R1), high resolution (R2) and full waveform (R3) modes in Metal Earth (Naghizadeh et al, 2019)

Parameter	Regional (R1) Mode	High-Resolution (R2) Mode	Full-Waveform (R3) Mode
Record length	12 or 16 s	12 s	12 s
Sample rate	2 ms	2 ms	2 ms
Spread size	15 km–0–15 km	All live (10–20 km)	All live (30–80 km)
Roll on/off	Yes	Yes	Yes
Source interval	50 m (4 sweeps); 12.5 m (1 sweep)	25 m (4 sweeps); 6.25 m (1 sweep)	As in R1
Receiver interval	25 m	12.5 m	25 m
Vibrator sweep	28 s, 2–96 Hz linear; 4 vibs;	28 s, 5–120 Hz + 3db/octave; 3 vibs;	As in R1

Table 3-2 summarizes the main processing steps and specific parameters that were used for processing the Metal Earth seismic data by Absolute Imaging Inc. to generate both post-stack and pre-stack migrated seismic sections (Naghizadeh et al, 2019).

3.4.3.2 The Metal Earth's seismic data interpretation

An appropriate image for interpreting major features on the R1 seismic section which is coincidence with the acquired gravity data along the transect is the curvelet enhanced data shown in Figure 3-10. The dotted blue lines illustrate more continuous reflectors, and the dotted red lines mark breaks in reflectors. Question marks in Figure 3-10 correspond to the area with lack of data or without any reflectors which could be related to the crooked areas of the Chibougamau transect.

The unreflective near-surface zones labeled as A, B, C, and D in Figure 3-10 are mainly interpreted to correspond to granitic, granodioritic bodies (plutons) intruded into the tonalitic rocks, some of which (A and B) do not outcrop on the surface. The approximately 5 km near-surface zone (primarily shown as green) has fewer reflections than the deeper zone labeled mid-crust on the section. The transition from the greenstone rocks in the near-surface to the mid-crust is interpreted as a decollement surface with unclear depth (Mint, 2017). There are some reflections along this boundary that reflect the syncline and anticline morphologies on the surface.

Within the mid-crust, the seismic images are characterized by gently dipping layers with thickness between 10 to 20 km (Mints, 2017).

Between the mid-crust and the crust-mantle boundary is a zone labeled lower crust on the interpreted section (Cook et al., 2010). Within the mid-crust, there is internal layering, which dips gently to the north. The dips are generally slightly steeper at shallow depths and flatten near

the boundary with the lower crust (Calvert and Ludden, 1999). The boundary between the mid- and lower crust was interpreted as a lower crustal decollement.

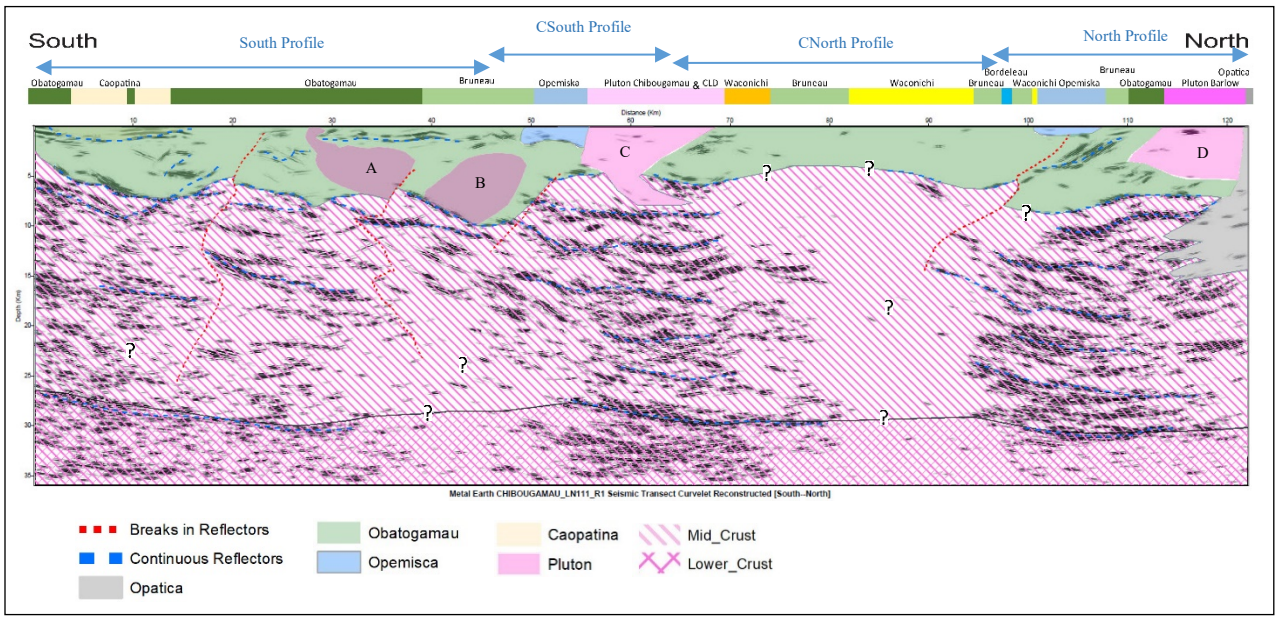

Figure 3-10. Interpretation of the Metal Earth Chibougamau R1 curvelet enhanced seismic transect. The blue arrows on top illustrate parts which are relevant for the South, CSouth, CNorth, North sections.

3.4.4 Physical properties

Changes in the density and magnetic susceptibility can reflect changes in the lithology, weathering, alteration and metamorphic grade as well as other processes like compaction. For example, higher density values are generally associated with rocks that are (i) more mafic than felsic, (ii) less weathered, (iii) higher in metamorphic grade, and compacted (Telford, et al. 1976). The magnetic susceptibility value of the rock reflects the opaque magnetic mineral content, so it is not useful in rock-type classification. However, the magnetic susceptibility can be used in mineral exploration studies as the alteration or metamorphism associated with mineralization events can create or destroy these iron minerals (Boroomand et al. 2015, Cisowski and Fuller 1987).

In this study, the density and average magnetic susceptibility values used were acquired from two published sources. Table 3-3 shows the values from Dion et al. (1992), where the values were measured from surface and borehole samples collected in the Chapais region. Some variation from the values in Table 3-3 is allowed to account for different levels of alteration and deformation.

The second source (Eshaghi et al., 2019) is a compilation of existing density and magnetic susceptibility measurements provided by different organizations: geological surveys and other research projects across the Superior Craton. In addition, the ME project's density and magnetic susceptibility measurements made prior to 2019, were added to the database. Eshaghi et al. (2019) include comprehensive statistics. Figures 3-11 and 3-12 represent the distribution of density and magnetic susceptibility measurements in major lithological units. The boxplots show there is overlap between different units and each unit has a reasonable broad range.

Conclusions draw from the two studies are as follows. Younger dykes (diabase) are mafic units with a strong magnetic signature and high-density values compare to other units. Granitic bodies have low values of density and a narrow range of variation. Sedimentary and metamorphic rocks also show a relatively low-density value. However, volcanoclastic packages can show a wide range of density values. In term of the magnetic susceptibility, felsic and intermediate igneous rocks, sedimentary rocks and metamorphic rocks generally show low responses. However, ultramafic igneous rocks and young dykes (diabase) exhibit strong magnetic responses.

As there is a limited number of samples involved in density and magnetic susceptibility measurements and results from the Metal Earth's study in Chibougamau area of interest, greater emphasis was given to the physical property values from the Table 3-3 when selecting values for the petrophysical models.

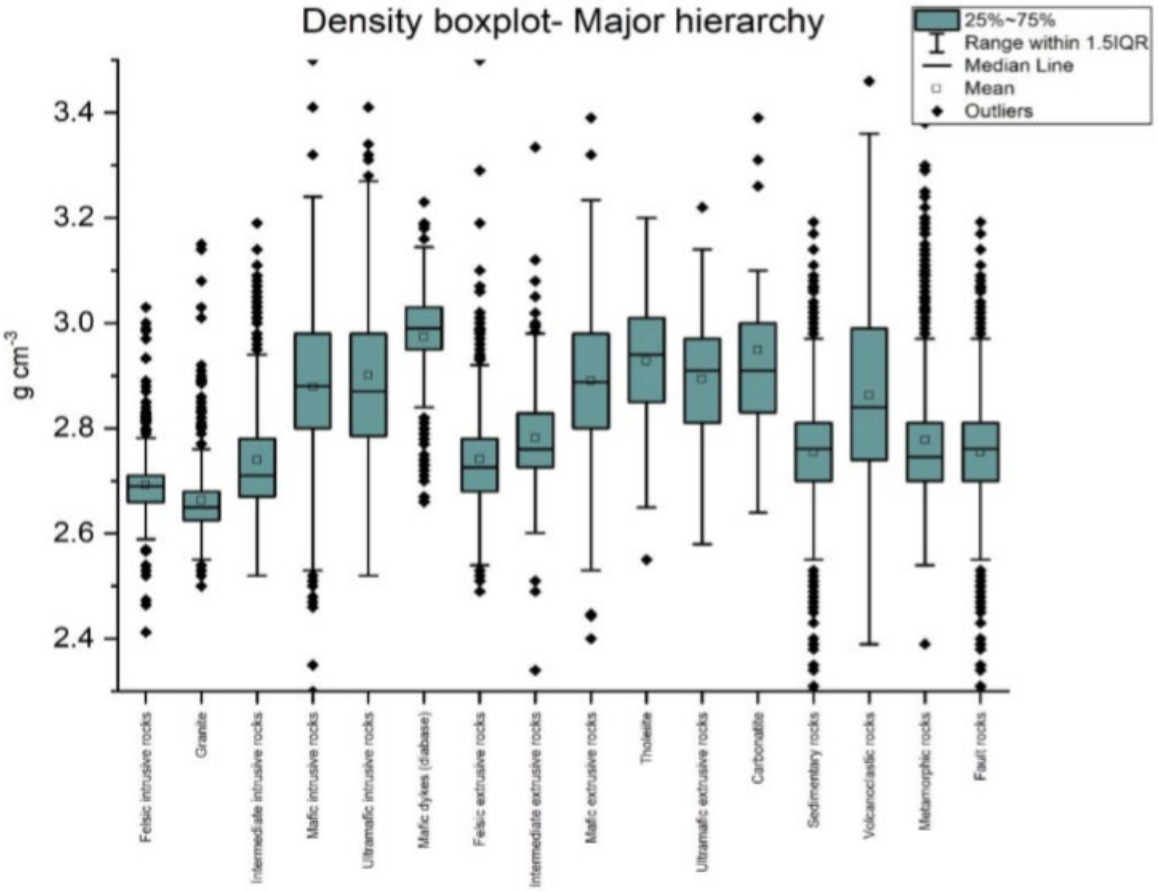

Figure 3-11. Boxplot analysis of density measurements represented by major lithological units (Eshaghi et al., 2019)

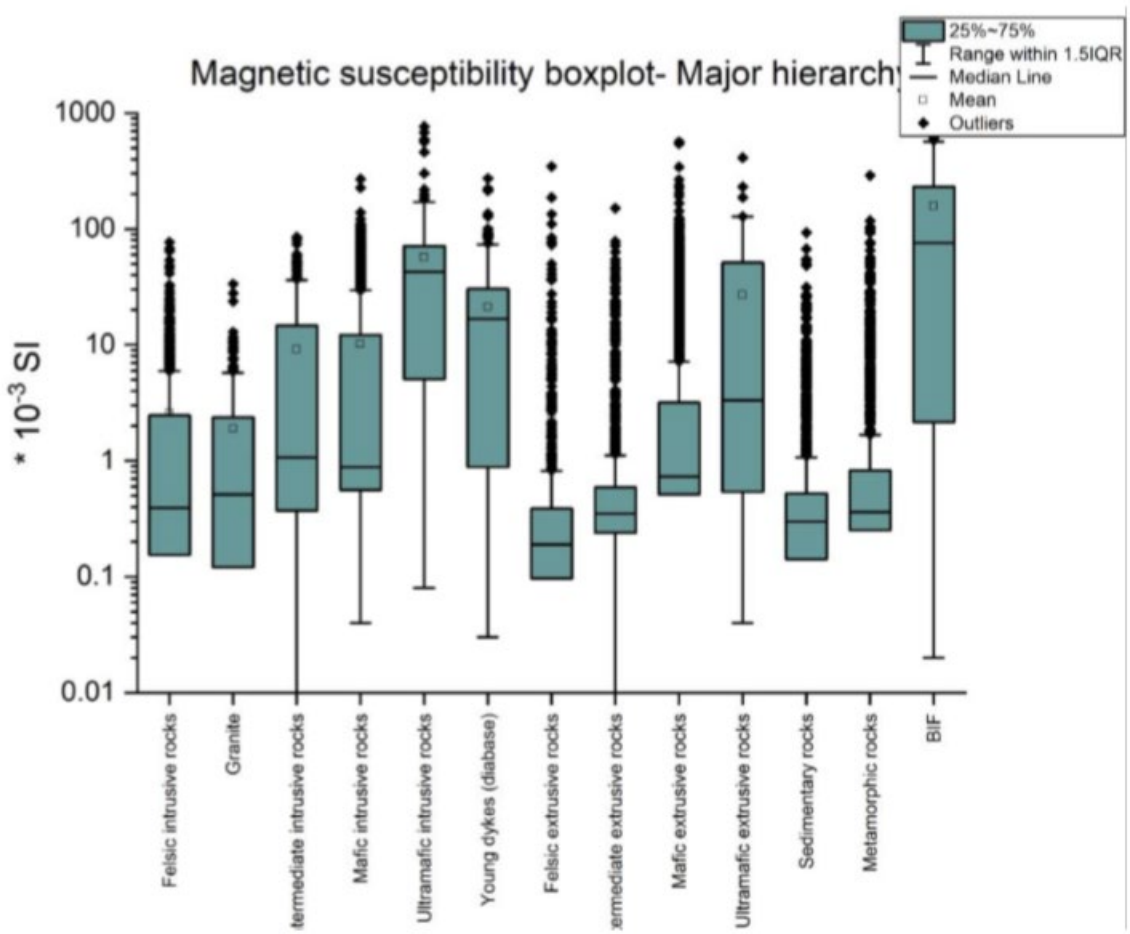

Figure 3-12. Boxplot analysis of magnetic susceptibility measurements represented by major lithological units (Eshaghi et al., 2019)

Table 3-2. Density and magnetic susceptibility measurements in Chapais area (Dion et al. 1992)

Lithology	N	Interval	Density (g/cm^3) Average ± SD	Magnetic susceptibility (*10^{-3}SI), interval
Opemisca Pluton				
Monzonite	6	2.62-2.64	2.63±0.008	0.01-0.8; 2.4-4.3
Presquile Pluton				
Tonalite	3	2.74-2.82	2.77±0.04	0.01; 0.2
Chibougamau Pluton				
Tonalite	12	2.60-2.73	2.67±0.04	0.01-2.3; 10-40
Diorite	21	2.73-3.06	2.93±0.1	0.01-2.3; 18-53
Opemisca Group				
Hauy Formation	10	2.72-2.97	2.87±0.07	0.1-0.5; 1.4-3.4
Stella Formation	4	2.71-2.76	2.74±0.02	0.1-0.5; 6.3-6.5
Daubree Formation	4	2.73-2.99	2.88±0.11	0.01; 0.6
cummings Complex				
Bourbeau Gabbro	9	2.83-3.05	2.97±0.07	0.01-0.6; 3-8
Ventures Gabbro	7	2.92-3.04	2.99±0.05	0.01-1.6; 12-45
Dunite	2	2.72-2.74	2.73	110; 190
Peridotite	6	2.66-2.79	2.73±0.04	72-130
Pyroxenite	5	3.12-3.27	3.21±0.06	0.8-8; 100
lac Dore Complex				
Anorthosite	2	2.99-3.00	2.99	0.01
Granophyre	1	2.61	2.61	0.2
Roy Group				
Blondeau Formation				
Sediments-tufs	24	2.66-2.91	2.79±0.06	0.01; 1.2
Andesite	8	2.75-2.83	2.79±0.04	0.01; 1.4
Gabbro dyke	6	2.85-2.98	2.90±0.05	17-100
Gilman Formation				
Basalt	11	2.80-3.23	2.99±0.13	0.01-1.6; 5-11
Gabbro	5	2.90-3.12	3.00±0.08	0.01-1.4; 6
Andesite	3	2.71-2.79	2.76±0.04	0.01; 0.4
Pyroclastic felsic	3	2.64-2.74	2.69±0.05	0.01; 0.1
Waconichi Formation				
Rhyolite	2	2.63-2.66	2.65	0.01; 0.1
Obatogamau Formation				
Basalt	27	2.73-3.10	2.95±0.12	0.01; 1.2
Gabbro	4	2.82-3.05	2.99±0.11	0.01; 1.4
Andesite	1	2.65	2.65	0.05
Chrissie Member	2	2.68-2.74	2.71	0.01; 0.5
Tonalitic Gneiss	22	2.56-2.77	2.67±0.05	---

3.5 2.5-D modelling

Figure 3-11 shows the four straight profiles used to approximate the crooked ME traverse overlain on the geology. The GM-SYS 2D software assumes that the geology is perpendicular to strike and extends an infinite difference either side of the profile. This is not the case, so we accounted for the finite strike length on either side of the profiles by using 2.5-D modelling. In the case of the CSouth and North profiles, the strike length on either side was set to 5 km, and for the South and CNorth profiles, it was set to 2 km in order to compute 2.5-D models. Geological strike angles not perpendicular to the traverse were not accounted for. The surficial geology map, geological sections, interpreted seismic section, petrophysical data acquired from surface, and the locations of surface magnetic contacts were used as constraints. The procedure for forward modelling of gravity and magnetics data was as follows (Olaniyan et al. 2014):

i) The magneto-stratigraphic contacts were used as surface controls; ii) The geological and seismic sections were used for assigning lithological boundaries in the subsurface; iii) Initial bodies were inserted consistent with the subsurficial lithological contacts specified above [in i) and ii)]; iv) physical properties were assigned to these units using the average density contrast values associated with each lithological unit, and then the response was computed; vi) I then adjusted the shape, position, the magnetic susceptibility and the density parameters within the acceptable variance of the location and physical properties until the misfit between the calculated response (solid line) and the measured fields (dotted line) was reduced as much as possible.

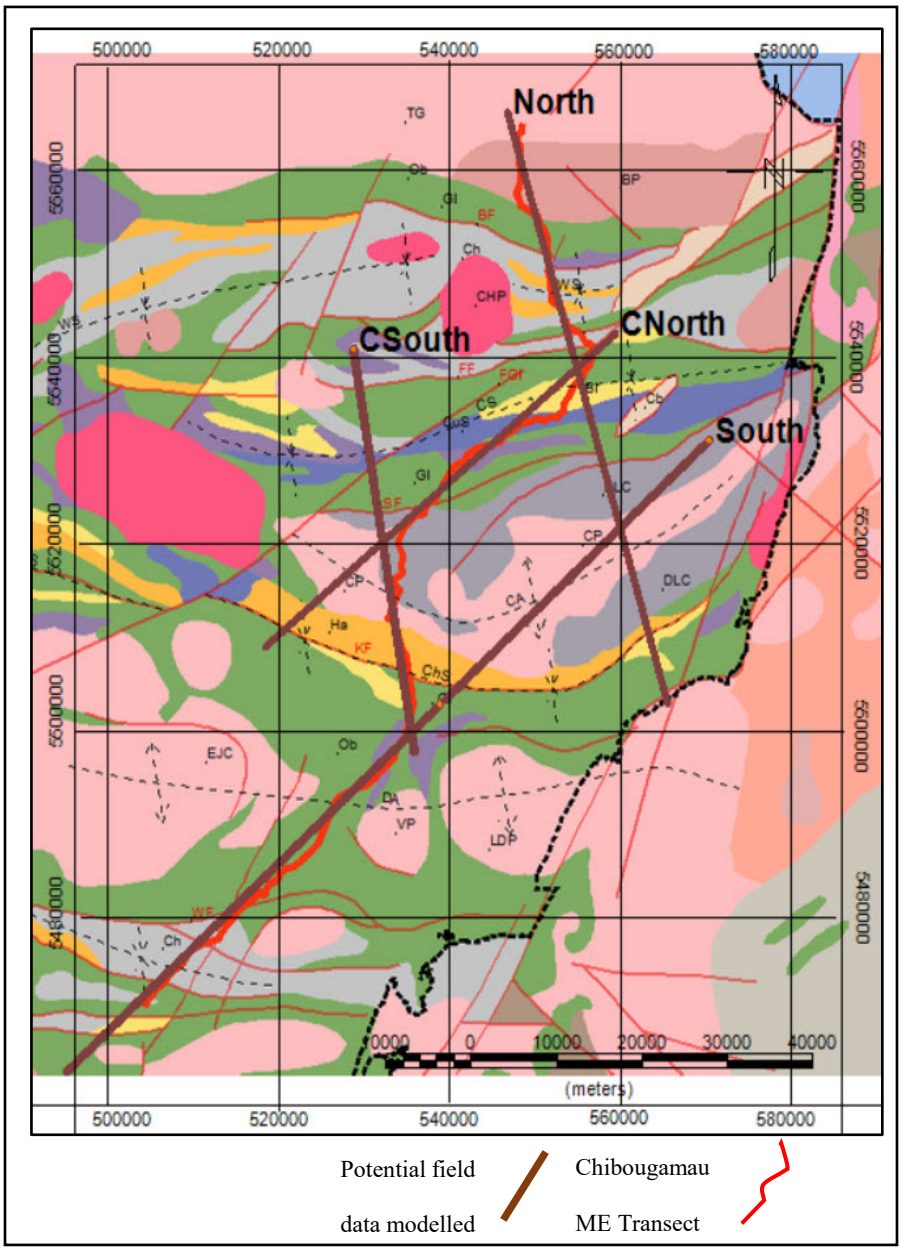

Figure 3-13. The location of the modelled sections on the geological map. See Figure 1-1 for abbreviations. Modified after (Montsion et al. 2017, Daigneault et al. 1990, Leclerc et al. 2008)

3.5.1 Profile South

Profile South is 103 km in length and trends in a SW-NE direction. The location of the profile has been selected so that the southernmost 44 km section coincides with the southern part of Chibougamau seismic transect, but the South profile continues further to the NE as there are public domain gravity and magnetic data available (Figure 3-11). From south to north, the geology can be summarized as including mafic porphyric volcanics of the Obatogamau Formation, the Caopatina Formation which consists of volcaniclastic and sedimentary rocks, mafic volcanics of the Gilman (Bruneau) Formation, sediments of the Opemisca formation, the tonalitic/dioritic Chibougamau pluton, and at the north end, the Dore Lac Complex with anorthosite and gabbro rocks. In detail, the Caopatina formation has a density of roughly 2.70 g/cm^3, so it exhibits a relative gravity low in the complete Bouguer corrected data (Figure 3-12). The Caopatina formation occurs as a sedimentary basin bounded by east-west striking longitudinal faults (Sharma et al. 1987). Within this broad low, a moderate gravity high in the middle of the sedimentary basin at 15 km is observed over a location where there is an outcrop of the mafic porphyric volcanics (Obatogamau formation) (2.85-2.95 g/cm^3 -- Table 3-3), which the Caopatina are interpreted to overlie. From 18 – 28 km along the profile in the Druillettes syncline, the gravity response increases approximately linearly. This could be interpreted as a thinning of the syncline, but I have also added and interpreted a deeper fractured zone in the Obatogamau formation, which has been assigned a density of 2.85 g/cm^3. If the density was greater and closer to the unfractured Obatogamau, the zone could be wider, but if less it would be narrower. This zone was inserted to be consistent with truncations evident in the seismic interpretations, and with a tectonic or deformation zone on the surface. There is some evidence for the fractured zone in the gravity data as a subtle inflection with short wave length from 25 to

29 km. The gravity continues to gradually increase from 28-40 km, but shows a dramatic decrease from 40-48 km, which is interpreted to be due to a deep plutonic body (2.75 g/cm^3) with a narrower 2 km wide tonalitic outcrop on surface consistent with the detailed geological map from 42 to 44 km. It is also consistent with a zone with no reflections on the seismic data. This pluton trends in the same east-west direction as the Eau Jaune Complex, the La Dauversière Pluton, and the Boisvert pluton, which all outcrop and are emplaced within the La Dauversière anticline (Figure 3-11). Further to the north, the gravity flattens with a sudden decrease from 53 to 55.5 km, which is consistent with a zone with no reflections on the seismic data that does not have any outcrop. However, there is an outcrop of granodioritic pluton close to the transect (~ 1 km in NW direction), which can be interpreted to be connected with it. Further to the north, there is another decrease in the gravity response which is interpreted to be associated with two adjacent geological features. The first is the Chapais syncline, which outcrops from 62-67 km, and comprises low-density sedimentary rocks (2.66 g/cm^3) of the Opemisca group (orange colour on the section) overlain by Cummings sills and Gilman formation. The Chapais syncline is bordered on the south by the Kapunapotagen fault (Charbonneau et al. 1983; Daigneault and Allard 1983, 1987). The second geological feature immediately to the north is the Chibougamau anticline from 67-90 km, in the section, this is represented by the low-density Chibougamau pluton (2.70 g/cm^3) composed of rocks of tonalite (2.76 g/cm^3) in the center of the pluton and the diorite on the border, with densities of 2.93 g/cm^3 (Dion et al. 1992). The gradual increase in gravity response to the north of the pluton is interpreted to be due to the decreasing thickness of the Chibougamau pluton, and diorite occurrences at the border. The gravity is consistent with a thickness of the northern thin portion of Chibougamau pluton of about 1 km, whereas the southern thick portion with a subvertical contact, could extend to about 7 km depth. At the north-

eastern end of the South profile, the geology comprises the Chibougamau anticline and the Lac Doré Complex, but the profile is semi-parallel to the anticlinal structure. Hence, the geometry and physical properties selected for the model will not be reliable, as the 2.5-D assumptions are not well satisfied. However, the high gravity values in this section are consistent with dense rocks composed of the layered intrusions of anorthosite, gabbro, pyroxenite (3.00 g/cm^3), which are part of the Lac Doré Complex. In some parts, there are some sharp drops in the gravity response, which have been explained by buried granophyre (2.61 g/cm^3) intruded into the Lac Doré Complex.

The total magnetic intensity data exhibits a relatively flat magnetic response across the South profile. However, there are some short wave length spikes in the Druillettes syncline that are interpreted to be due to mafic intrusions and diabase dykes which are consistent with the magnetic map interpretations (Figure 3-4). Between 58 and 67 km along the profile, the Cummings sills, and mafic intrusions which underlay the sedimentary rocks of the Opemisca group have been interpreted as the source of some short wavelength fluctuations in the magnetic responses. The highest magnetic response along the South profile belongs to two sharp anomalies over the Lac Doré Complex in the north-eastern end of the profile, which are modelled as two subvertical mafic intrusions with high magnetic susceptibilities. Small changes in the shapes of these bodies could result in better agreement between the model and measured data, but the precise geometries of these magnetic bodies were not considered an important part of this project.

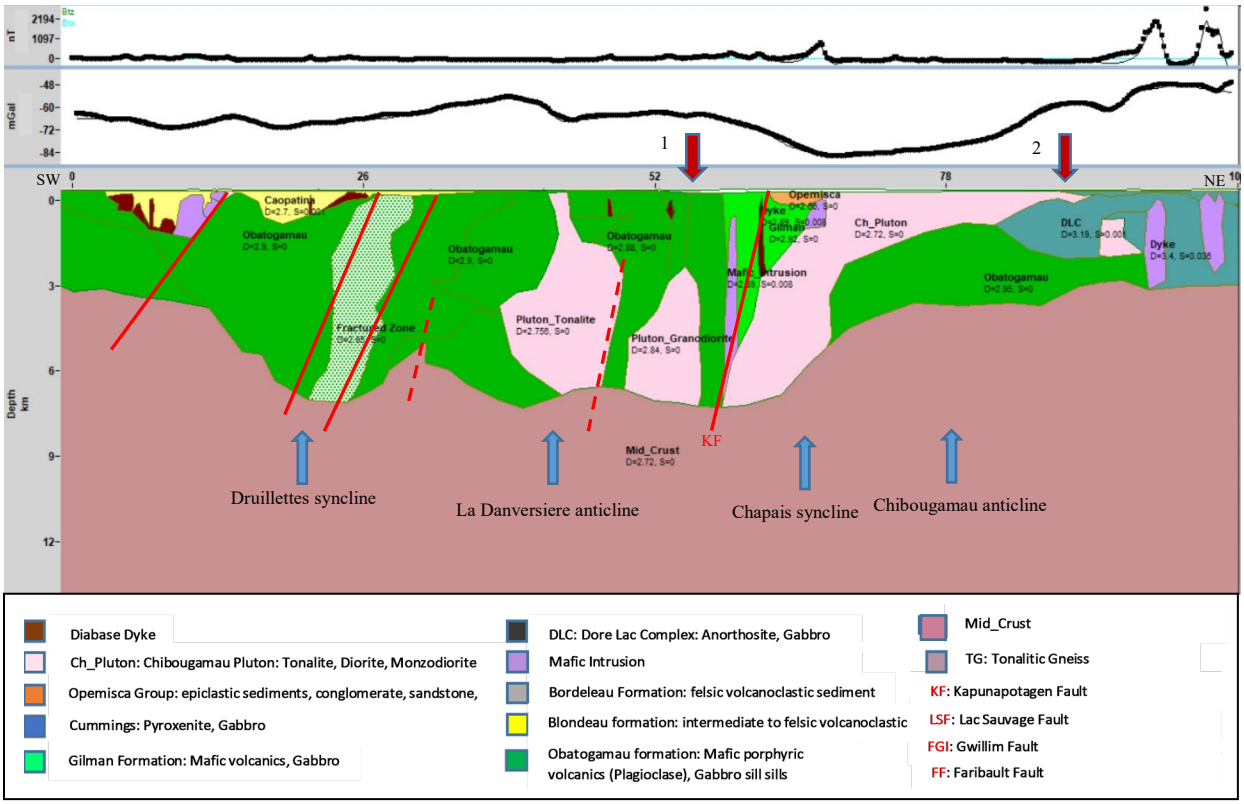

Figure 3-14. 2.5-dimensional geological model for profile South (bottom) and the corresponding magnetic (top) and gravity (middle) data from the compilation of Metal Earth's and GSC's data. The measured data is the thick dotted line and the forward model data is the thin solid line. D-density (g/cm^3), S-susceptibility (SI). Seismic constraints apply only between 12 - 56 km along the profile. The top red arrows show the location of the intersection of the South and CSouth profiles (#1), South and North profiles (#2). The blue arrows show the location of anticlines and synclines.

3.5.2 Profile CSouth

Profile CSouth is 44 km in length and trends in an approximate S-N direction. The location of the profile has been selected to include constraints from part of the Chibougamau seismic transect between 45 and 66 km. The CSouth profile extends further to the N and S as there are public domain gravity and magnetic data (Figure 3-11). From south to north (Figure 3-13), the surface geology can be summarized as including volcanic rocks of the Obatogamau and the Gilman formations, the Opemisca group with sandstones, siltstones, and polygenic conglomerates occupied the Chapais syncline, the tonalitic/dioritic Chibougamau pluton, the Lac Sauvage fault at the southern limit of Chibougamau syncline, which is occupied by the Roy group, including the Cummings Complex sills and the overlying Blondeau sediments in the northern part. At the northern end of the profile, the Faribault fault demarcates the southern limit of the Waconichi tectonic zone (the Waconichi anticline) composed of the Bordeleau sediments and mafic intrusions.

In detail, the first 7.7 km is covered by mafic rocks, with a rough density of 2.8 g/cm^3, of the Obatagamau and the Gilman formations, which exhibit a flat gravity response in the complete Bouguer corrected data. To the north of the Kapunapotagen fault is the Opemisca group with a density of roughly 2.66 g/cm^3 (and interpreted to overlie the Gilman formation) and then further to the north, the southern corner of the Chibougamau pluton. These lower density rocks correspond to a gradual decrease in gravity response. The lowest gravity response along the CSouth profile is interpreted to be due to tonalitic/dioritic rocks (2.65 g/cm^3) in the Chibougamau anticline, which is consistent with an area without reflectors in the seismic profile. From ~ 9.5 to 25.5 km along the profile, the Chibougamau pluton occupies the Chibougamau

anticline, where the thickness of the portion north of 16 km is about 800 m and overlies the Obatogamau formation (2.95 g/cm^3), whereas the southern thick portion could extend to about 8 km. There is a flat part with some short wave length fluctuations in gravity data from 20.5 to 25.7 km, which is interpreted to be due to slight changes in the thickness of the Chibougamau pluton in the thin part. The smooth gradual increase in gravity response from 25.7 km to 27 km is interpreted to be due to the gradual disappearance of the Chibougamau pluton, and the reverse movement of the Lac Sauvage fault which makes a thin part of the Waconichi formation with a density of roughly 2.8 g/cm^3. Further to the north toward 29.5 km, there is a steeper increase in gravity data from -46.5 to -39 mGal, which is interpreted to be due to the increase in the thickness of the denser lithologies, such as the Obatogamau and the Gilman formations (2.95-3.00 g/cm^3) with the depth extent not exceeding 3600 m. The Chibougamau syncline is bounded between two east-west oriented faults (the Lac Sauvage fault to the south, and the Faribault fault to the north), and the dominant lithologies are the Cummings Complex sills and the assemblage of Roy Group rocks (the density for these rocks vary between 2.78 and 3.00 g/cm^3) indicated a broad and smooth high gravity response with a moderate decrease over sedimentary rocks of Blondeau formation with densities of roughly 2.78 g/cm^3. The far north of the profile shows a gradual smooth decrease in Waconichi tectonic zone with sedimentary rocks of Bordeleau formation and mafic intrusions of the Cummings complex.

The total magnetic intensity data is moderately flat along the first 30 km. There are some short wave length spikes on the northern flank of the Chibougamau anticline, which are modelled as mafic intrusions and dykes with higher magnetic susceptibilities than surrounding rocks. The highest magnetic response is recorded over the Cummings sills and mafic intrusions with high magnetic susceptibilities in the Chibougamau syncline. There is drop in magnetic data form ~32

km to the end of the profile, which is interpreted to be due to sedimentary rocks in the Chibougamau syncline (Blondeau formation), and in the Waconichi anticline (Bordeleau formation) with low magnetic susceptibilities. Also, a highly fractured area in the Waconichi tectonic zone could result in the destruction of magnetic minerals.

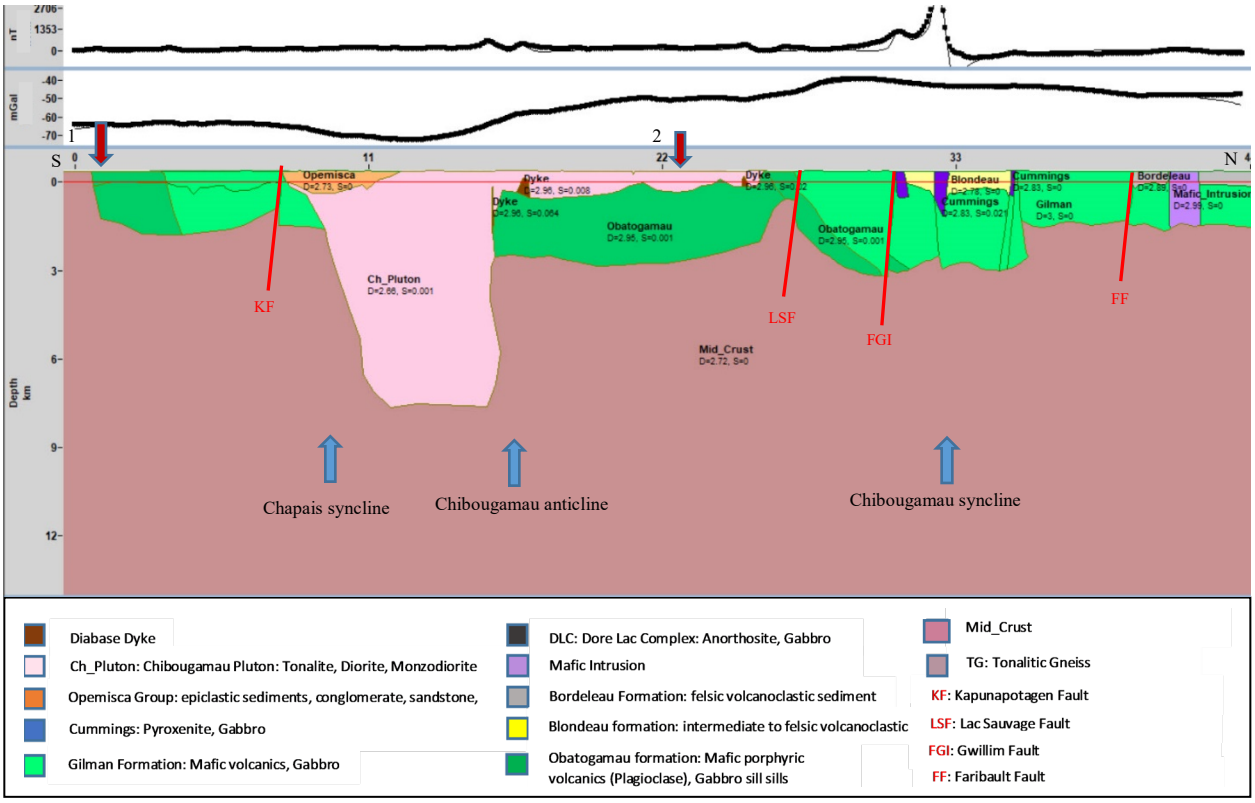

Figure 3-15. 2.5-dimensional geological model for profile CSouth (bottom) and the corresponding magnetic (top) and gravity (middle) data from the compilation of the Metal Earth and GSC data. The measured data is the thick dotted line and the forward model data is the thin solid line. D-density (g/cm^3), S-susceptibility (SI). Seismic constraints apply only from 3 – 24 km of the profile. The top red arrows show the location of the intersection of the South and CSouth profiles (#1), CNorth and CSouth profiles (#2). The blue arrows show the location of anticlines and synclines.

3.5.3 Profile CNorth

Profile CNorth is 54 km in length and trends in an approximate SW-NE direction. The location of the profile has been selected in order to use the seismic section from its 65 km location to the 96 km location as constraints for the potential field model. However, the CNorth profile continues further to the NE and SW as there are public domain gravity and magnetic data available (Figure 3-11). From SW to NE (Figure 3-14), the geology can be summarized as including basalt and andesitic basalt rocks of the Gilman formation, sedimentary rocks of the Opemisca formation, the Chibougamau pluton with tonalitic, dioritic, and granodioritic rocks, mafic volcanic and intermediate rocks of the Gilman formation, mafic to ultramafic intrusions, Cummings sills overlying the Gilman formation, Blondeau sediments, and at the north-eastern end of the profile the Bordeleau sediments are separated by the Faribault fault. In detail, there are two adjacent geological features along the first 6 km of the profile which result in a steep and linear decrease in the gravity response. The first one is the Opemisca sedimentary basin with a density value of roughly 2.66 g/cm^3, which is interpreted to overlie the Chibougamau plutonic body and the Gilman formation. The Chibougamau pluton is a Tonalitic/dioritic intrusion with 2.65 – 2.70 g/cm^3 and a subvertical contact that could extend to about 9 km depth. The gradually moderate increase in gravity response from 6 to 22 km is interpreted to be due to the gradual decreasing thickness of the Chibougamau pluton, and diorite occurrences on the border of it. There are some short wave fluctuations in the gravity response along the thin northern portion of the Chibougamau pluton, which is interpreted as firstly topographic fluctuations of the border between plutonic body and the underlying mafic rocks of the Obatogamau formation, and secondly some hidden mafic intrusions and mafic rocks of the Lac Doré Complex (which have a broad gravity anomaly). Crossing the Lac Sauvage fault further to the north is the southern

limit of the Chibougamau syncline and a dramatic increase in the thickness of the assemblage of Roy group rocks (Gilman and Obatogamau formations) with roughly density value 2.9 -3 g/cm^3. These result in a generally gradual increase in gravity response from 22 to 27.7 km. It should be mentioned that the sharp change in the thickness of the Roy group rocks is consistent with the seismic interpretations, but the profile is semi-parallel to the geological structure, and the transect is crooked in this area. Therefore, the geometry selected for the model, and the seismic interpretation will not be reliable, as the 2.5D assumptions are not well satisfied. The gradual increase in gravity response continues toward 32.7 km which is interpreted to be due to the mafic intrusive body with a density value of roughly 3.2 g/cm^3 which outcrops on the surface. A slight low in the gravity data at 29.5 km is observed over a location where there is an outcrop of basalt and andesitic basalts of the Gilman formation (2.7 – 2.9 g/cm^3 -- Table 3-3), which overlies the previously mentioned mafic intrusion body. About a further 2 km to the north, the flatter gravity response is interpreted to be due to basalt/andesitic basalt rocks of the Gilman formation which outcrop. Between 34.5 to 45 km is generally flat with some slight increases and decreases. The increases are interpreted to be due to the pyroxenite, dunite, and peridotite rocks of the Cummings sills with density values 2.7 - 2.9 g/cm^3 (Table 3-3) which has a number of outcrops on surface. The slight decreases are related to intermediate to felsic volcanoclastic sediments of the Blondeau formation (2.76 g/cm^3) which also outcrops on surface. North of the Faribault fault, the gravity is reduced in the Waconichi tectonic zone as a consequence of the less dense sedimentary rocks of the Bordeleau formation.

The total magnetic intensity data exhibited an overall moderate flat along the first ~34 km. At 8, 13 and 19 km here are some increases in magnetic response on the northern flank of Chibougamau anticline, which are modelled as buried mafic intrusions and dykes with higher

magnetic susceptibilities than surrounded rocks. These anomalies are consistent with interpreted magnetic lineaments in Figure 3-4. The other alternative for these features is hidden mafic intrusions and mafic rocks of the Lac Doré Complex with high magnetic susceptibility content. The largest magnetic responses are recorded over the Cummings sills and mafic intrusions with high magnetic susceptibility content in the Chibougamau syncline from 34 to 46.5 km. Within these highs, the local lows are associated with sedimentary basins containing the Blondeau formation (low magnetic susceptibility). There is a drop in magnetic response from ~46.5 km to the end of the profile, which is interpreted to be due to two packages of low magnetic susceptibility sedimentary basins; one in the Chibougamau syncline (Blondeau formation), and the other in the Waconichi anticline (Bordeleau formation) with low magnetic susceptibility content. The highly fractured area in the Waconichi tectonic zone could also result in magnetic material being destroyed.

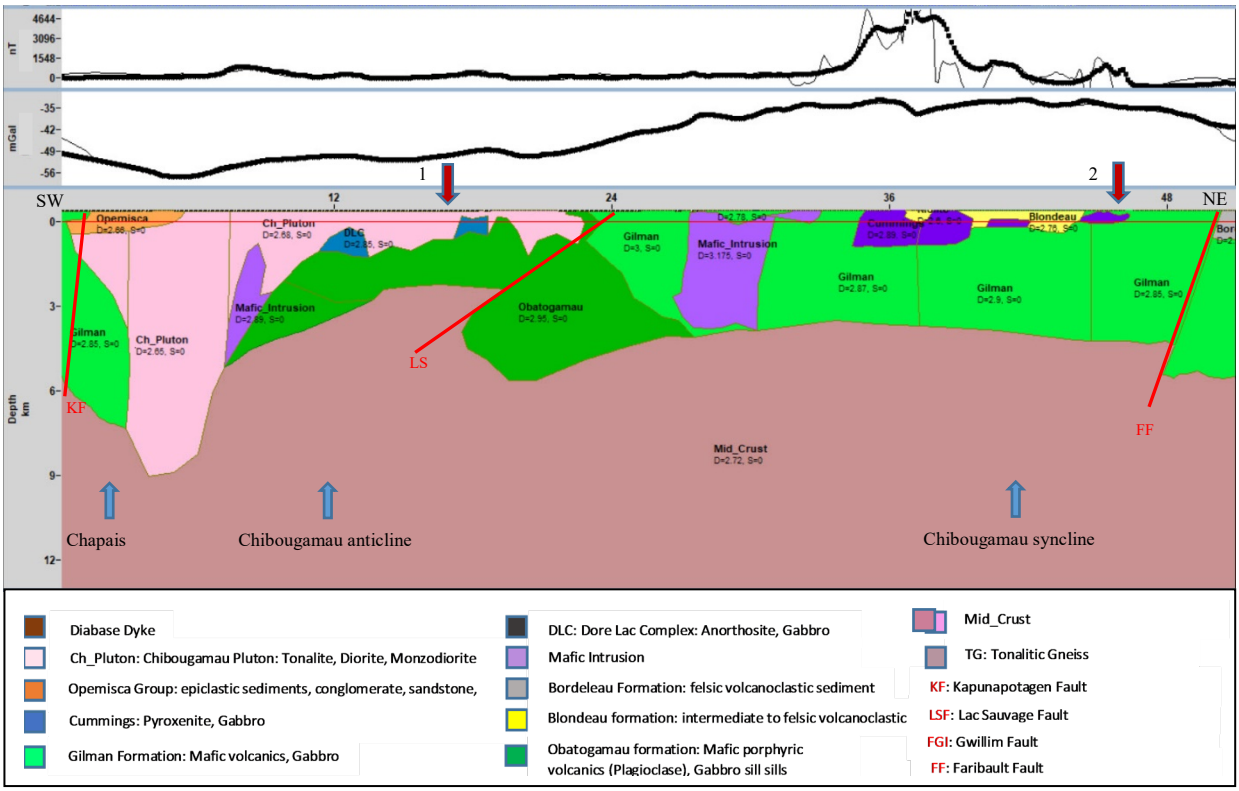

Figure 3-16. 2.5-dimensional geological model for profile CNorth (bottom) and the corresponding magnetic (top) and gravity (middle) data from the compilation of Metal Earth and GSC data. The measured data is the thick dotted line and the forward model data is the thin solid line. D-density (g/cm^3), S-susceptibility (SI). Seismic constraints apply only from 17 – 48 km of the profile. The top red arrows show the location of the intersection of the CNorth and CSouth profiles (#1), CNorth and North profiles (#2). The blue arrows show the location of anticlines and synclines.

3.5.4 Profile North

Profile North is 66 km in length and runs from south to north. The location of the profile has been selected so that the northernmost 28 km section coincides with the northern part of Chibougamau seismic transect, but the North profile continues further to the south as there are public domain gravity and magnetic data (Figure 3-11). From south to north (Figure 3-15), the geology can be summarized as including volcanic rocks of the Obatogamau and the Gilman formations, sandstones, siltstones, and polygenic conglomerates of the Opemisca group occupying the Chapais syncline, the Dore Lac Complex with anorthosite, gabbro rocks, the tonalitic/dioritic Chibougamau pluton, the Lac Sauvage fault at the southern limit of the Chibougamau syncline occupied by the Cummings Complex sills and the assemblage of Roy Group rocks overlain by Blondeau sediments. In the northern half of the profile, the Faribault fault demarcates the southern limit of the Waconichi tectonic zone (the Waconichi anticline), which is composed of the Bordeleau sediments and mafic intrusions, the Waconichi syncline (WS) is occupied by sedimentary rocks of the Opémisca Group and is bounded by longitudinal east-west faults. At the north of the profile is the Barlow pluton with tonalitic/granodioritic rocks and then at the extreme north the Opatica plutonic belt with tonalitic gneiss rocks. In detail, the first 6.5 km is covered by mafic rocks of the Obatagamau and the Gilman formations (~2.8 g/cm^3), which exhibit a smooth gravity response with a slight decrease attributed to an increase in the thickness of the Blondeau sediments with a rough density of 2.68 g/cm^3. Crossing the east-west trending Kapunapotagen fault with a southerly dip and a reverse movement, is the Opemisca group (~2.66 g/cm^3) which is overlain by Gilman formation and anorthosite, gabbro rocks of the Dore Lac Complex (2.98 g/cm^3) below and to the north, resulting in a gradual increase in gravity response to the north. The lowest gravity response along the North profile is

interpreted to be due to tonalitic/dioritic rocks (2.65 g/cm^3) in the Chibougamau pluton and anticline which is evident from 10-15 km along the profile. Both of the southern and northern limbs of the Chibougamau pluton with a subvertical contact could extend to about 7.7 km. The northern portion of the Chibougamau pluton overlies the Obatogamau and Gilman formations (2.95-2.97 g/cm^3) so there is a gradual increase in gravity response from 18 km to 21 km along the profile. There is a flat part of the gravity response with some short wavelength fluctuations from 21 to 30.3 km, which is interpreted as changes in the thickness of Roy group rocks. Further to the north, there is a gravity peak at 32.8 km, which is interpreted to be due to Cummings sills (2.9-3.05 g/cm^3) which is supported by a mapped outcrop in the Chibougamau syncline. The outcrop of Blondeau sediments from 32.8-34.8 km shows a drop in gravity response. At 45.3 km, there is a gradual decrease in the gravity response which is interpreted to be due to not only the decrease in the thickness of the denser lithologies, such as the Gilman formations (2.9-2.95 g/cm^3) with vertical extension not exceeding 2300 m, but also the occurrence of sedimentary rocks of the Opémisca Group with lower density than surrounding rocks in the Waconichi syncline. There is a gravity high from 43.1-44.3 km which is interpreted to be due to mafic intrusions with high density in the Waconichi syncline. At 50.1 km, the gravity starts to decrease. Although there is an interpreted reverse movement of the Barlow fault which increases the thickness of the denser lithologies, such as the Obatogamau and Gilman formations with a rough density 2.85-2.95 g/cm^3, the gravity actually decreases. This is likely the impact of the deep and less dense tonalitic/granodioritic rocks of the Barlow pluton (2.69 g/cm^3) and the tonalitic gneiss rocks of the Opatica plutonic belt (2.66 g/cm^3) which are at the extreme end of the profile but interpreted to extend to great depth.

The total magnetic intensity data appear moderately flat along the first 29 km. There are some short wave length spikes on both the northern and the southern flanks of the Chibougamau anticline, which are modelled as mafic intrusions and dykes with higher magnetic susceptibilities than surrounding rocks. The highest magnetic response is recorded over the Cummings sills and mafic intrusions with high magnetic susceptibility content in the Chibougamau syncline. There is a drop in magnetic data from 33 to 42.2 km, which is interpreted to be due to the two sedimentary packages; one in the Chibougamau syncline (Blondeau formation), and the other in the Waconichi anticline (Bordeleau formation). There is a strong magnetic anomaly from 42.7 to 44.4 km which is consistent with a mafic intrusive body with a higher magnetic susceptibility than surrounded sediments in the Waconichi syncline.

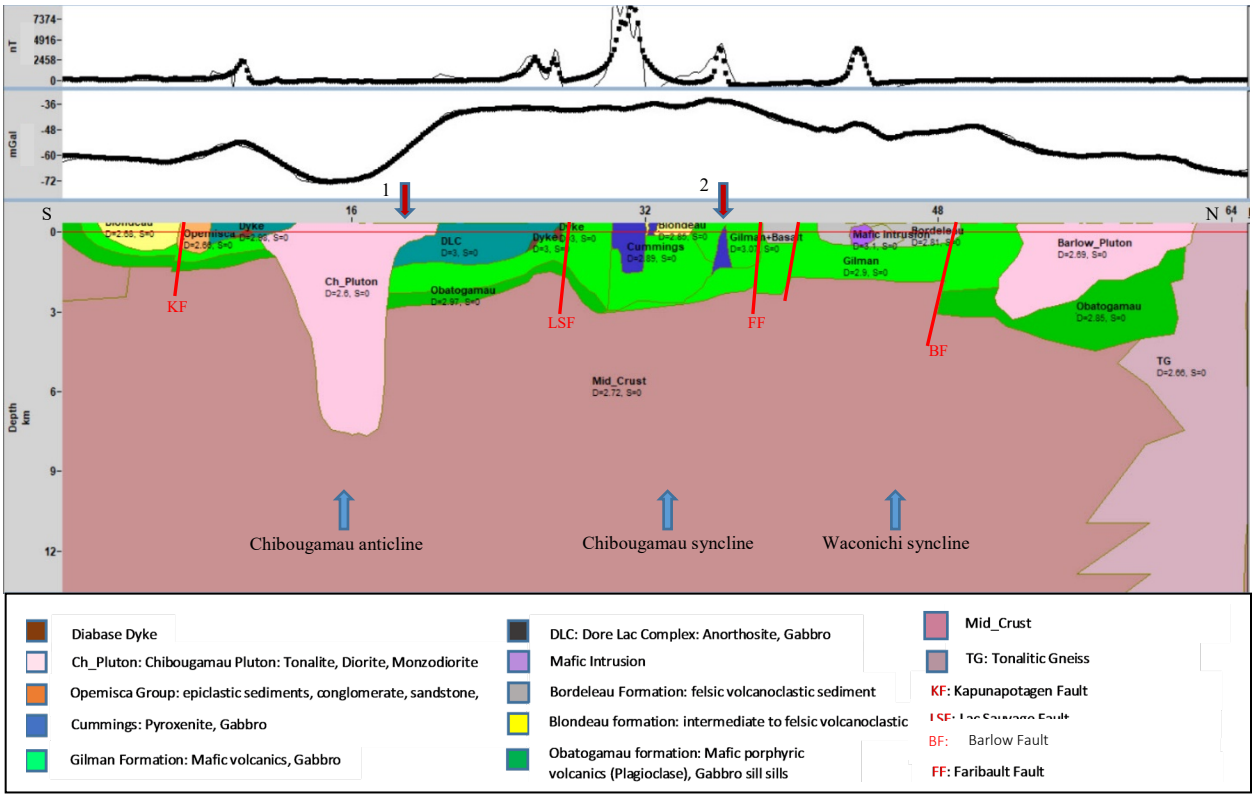

Figure 3-17. 2.5-dimensional geological model for profile North (bottom) and the corresponding magnetic (top) and gravity (middle) data from the compilation of Metal Earth's and GSC's data. The measured data is the thick dotted line and the forward model data is the thin solid line. D-density (kg/m^3), S-susceptibility (SI). Seismic constraints apply only from 37.5 – 65.5 km of the profile. The top red arrows show the location of the intersection of the South and North profiles (#1), CNorth and North profiles (#2). The blue arrows show the location of anticlines and synclines.

3.6 Conclusion

When modelling the potential field data, I found the gravity data modelling was helpful in adjusting the shape and densities of features at depth and could resolve the geometry of some features such as plutonic bodies (for example the Barlow and Chibougamau plutons) which are transparent in seismic sections. However, when the profiles are sub-parallel to the geological structures, the geometry and physical properties selected for the model will not be reliable, as the 2.5-D assumptions are not well satisfied. In these cases, more reliable results will be obtained with 3D modelling.

The magnetic data was useful in adjusting the shape and magnetic susceptibility of geological bodies with a strong magnetic content contrast with surrounding rocks. These bodies were primarily mafic intrusions and dykes. However, I did not put much time into modelling these magnetic bodies it was difficult and primarily involved adjusting very near surface features and adding in remanent magnetization which was not considered an important part of this project. The modelling was made more difficult by (i) a shortage of petrophysical data at depth, (ii) changes in the physical properties along a profile and with depth within one geological formation, (iii) lack of constraints in transparent areas of the seismic profiles and where the seismic profile was crooked and the imaging poor, (iv) uncertainty in the depth of the transition between the upper crust and the mid-crust. However, the gravity and magnetic modelling were able to provide some guidance as to the subsurface structures in the seismically transparent areas, albeit with less confidence than in areas where there are seismic constraints.

The magnetic interpretation map helped when reinterpreting the boundary of the Chibougamau pluton and Lac Dore complex which was also used to define the density contrast boundary and was therefore useful in data modelling.

In the La Danversiere anticline (the south profile), a new pluton (with no outcrop) was modelled at depth, which impacts the seismic interpretation and could be interpreted to be connected with an outcrop of granodioritic pluton close to the transect to the NW.

In the southern part of the South profile, in the Druillettes syncline, a fractured zone is interpreted in the Obatogamau formation, relevant to the seismic interpretation and to the deformation zone observed on surface. This area could be interesting for further mineral exploration studies.

Potential-field data modelling can be used to define the shape of plutonic bodies, for example, it was used to model the thickness of the Chibougamau pluton, and the shape of the Barlow pluton at depth, which might be relevant in future mineral exploration studies.

These models should be revised when the results of the magnetotelluric studies, high-resolution R2 seismic data, detail seismic interpretation of R1 seismic data, and detail geological studies become available. When all this information is integrated, it might be possible to achieve the goals of the Metal Earth project and understand the processes that result in metallogenesis. Specific guidance that the gravity and magnetic can provide is the sense and throw on some of the major structures in the area and the size and locations of the major plutons.

Chapter 4

4 References

Allard, G.O. 1976. Doré Lake Complex and its importance to Chibougamau geology and metallogeny. Ministère des Richesses Naturelles du Québec, DP 368.

Allard, G. O., and Gobeil, A. 1984. General geology of the Chibougamau region. In Chibougamau-stratigraphy and mineralization. Edited by J. Guha and E. H. Chown. The Canadian Institute of Mining and Metallurgy, Special Volume 34, pp. 5-20.

Baker, D. 1980. The metamorphic and structural history of the Grenville Front near Chibougamau, Québec. Ph.D. thesis, University of Georgia, Athens, GA.

Benn, K., Sawyer, E.W., and Bouchez, J.-L. 1992. Orogen parallel and transverse shearing in the Opatica belt, Quebec: Implications for the structure of the Abitibi Subprovince, Canadian Journal of Earth Sciences, 29, pp. 2429-2444.

Boroomand, M.A., Safari, A., and Bahroudi, A., 2015. Magnetic susceptibility as a tool for mineral exploration (Case Study: Southern of Zagros Mountains). International Journal of Mining and Geo-Engineering, 49, pp. 57-66.

Calvert, A. J., and Ludden, J. N. 1999. Archean continental assembly in the southeastern Superior Province of Canada. Journal Tectonics, 18, pp. 412-429.

Castro, A. 1986. Structural pattern and ascent model in the Central Estremadura batholith, Hercynian belt, Spain. Journal of Structural Geology, 8, pp. 633-645.

Charbonneau, J. M., Picard, C., and Dupuis-Herbert, L. 1983. Géologie des unités stratigraphiques affleurant dans les cantons de Daubrée, Dolomieu, Saussure et La Ribourde, district de Chibougamau.

In Rapports d'étape des travaux en cours à la division du Précambrien. Ministère de 1'Energie et des Ressources du Québec, ET 82-01, pp. 1-68.

Cisowski, S.M. and Fuller, M., 1987. The generation of magnetic anomalies by combustion metamorphism of sedimentary rock, and its significance to hydrocarbon exploration. GSA Bulletin 99, pp. 21-29.

Cooper, G. R. J., and D. R. Cowan, 2006. Enhancing potential field data using filters based on the local phase: Computers & Geosciences, 32, pp. 1585-1591.

Cook, F.A., White, D.J., Jones, A.G., Eaton, D.W.S., Hall, J., Clowes, R.M., 2010. How the crust meets the mantle: Lithoprobe perspectives on the Mohorovičić discontinuity and crust–mantle transition. Canadian Journal of Earth Sciences, 47 (4), pp. 315–351.

Daigneault, R. 1982. Demie nord du canton de McKenzie. Ministère de 1'Energie et des Ressources du Québec, DP 82-08.

Daigneault, R., and Allard, G. O. 1983. Stratigraphie et structure de la région de Chibougamau. In Statigraphie des ensembles volcanosédimetaires archéens de l'Abitibi: Etat des connaissances. Ministère de 1'Energie et des Ressources du Québec, DV 83-13, pp. 1-18.

Daigneault, R., and Allard, G. O. 1984. Évolution tectonique d'une portion du sillon de roches vertes de Chibougamau. In Chibougamau-stratigraphie and minéralisation. Edited by J. Guha and E. H. Chown. The Canadian Institute of Mining and Metallurgy, Special volume 34, pp. 212- 228.

Daigneault, R., and Allard, G. O. 1987. Les cisaillements E-W et leur importance stratigmphique et métallogénique, région de Chibougamau:In Études géoscientifiaues récentes. Séminaire d'information 1987. Ministère de 1'Energie et des Resources du Québec, DV 87-25, pp. 57-73.

Dentith, M., Mudge, S. T. 2014. Geophysics for the Mineral Exploration Geoscientist., Cambridge University Press. 454 p.

Daigneault, R., St-Julien, P., and Allard, G.O. 1990. Tectonic evolution of the northeast portion of the Archean Abitibi greenstone belt, Chibougamau area, Quebec: Canadian Journal of Earth Sciences, 27, pp. 1714–1736.

Dimorth, E., Muir, W., Rocheleau, M., Archer, P., Jutras, M., Piche, M., Simoneau, P., Carignan, J., Chown, E. H., Guha, J., Goulet, N., Allard, G. O., Franconi, A., and Gobeil, A. 1983. Stratigraphie et évolution du bassin de transition entre les Groupes de Roy et d'opémisca, région de Chibougamau-Chapais. Stratigraphie des ensembles volcano-sédimentaires de l'Abitibi: Etat des connaissances. Ministère de 1'Energie et des Ressources du Québec, DV 83-1 1, pp. 21-35.

Dion, D.J., Morin, R., and Keating, P., 1992. Synthese geologique et geophysique de la region de Chapais: portion orientale de la ceinture de I'Abitibi Quebecoise. Canadian Journal of Earth Sciences, 29, pp. 314-327.

Eshaghi, E., Smith, R. S., Ayer, J., 2019. Petrophysical characterisation (i.e. density and magnetic susceptibility) of major rock units within the Abitibi Greenstone Belt. Laurentian University Mineral Exploration Research Centre, publication number MERC-ME-2019-144.

Gobeil, A., and Racicot, D. 1983. Carte lithostratigraphique de la région de Chibougamau au 11250 000. Ministère de 1'Energie et des Ressources du Québec, MM 83-02.

Geosoft Inc., 2015. montaj gravity and terrain correction how-to Guide, available: http://updates.geosoft .com/downloads/files/how-to guides/Gravity%20and%20Terrain%20Correction%20Formulas.pdf, [Date Accessed: 11th June 2015]

Henry, R. L., and Allard, G. 0. 1979. Formation ferrifère du Lac Sauvage, cantons de McKenzie et de Roy, région de Chibougamau. Ministère des Richesses maturelles du Québec, DPV 593.

Hood, P. J., 1965, Gradient measurements in aeromagnetic surveying, Geophysics, 30, pp. 891-902.

Hrouda, F. and Kapička, A., 1986. The effect of quartz on the magnetic anisotropy of quartzite. Studia Geophysica et Geodaetica 30, pp. 39-45.

Kearey, P., Brooks, M. and Hill, I. 2012. An introduction to geophysics exploration; Blackwell Science, Oxford, 268p.

Krogh, T. E. 1982. Improved accuracy of U-Pb zircon ages by the creation of more concordant systems using air abrasion technique. Geochimica et Cosmochimica Acta, 46, pp. 637-649.

Leclerc, F., Bedard, J.H., Harris, L.B., Goulet, N., Houle, P., Roy, P. 2008. Nouvelles subdivisions de la Formation de Gilman, Groupe de Roy, région de Chibougamau, Sous-province de l'Abitibi, Québec: résultats préliminaires. Commission géologique du Canada; Recherches en cours 2008-7, 20 p.

Leclerc, F., Bedard, J.H., Harris, L.B., McNicoll, V., Goulet, N., Roy, P., Houle, P. 2011. Tholeiitic to calc-alkaline cyclic volcanism in the Roy Group, Chibougamau area, Abitibi Greenstone Belt, Revised stratigraphy and implications for VHMS exploration: Canadian Journal of Earth Sciences, 48, pp. 661-694.

Ludden, J., Hynes, A., 2000. The Lithoprobe Abitibi–Grenville transect: two billion years of crust formation and recycling in the Precambrian Shield of Canada: Canadian Journal of Earth Sciences, 37, pp. 459-476.

Mereu, R.F. 2000. The complexity of the crust and Moho under the southeastern Superior and Grenville Provinces of the Canadian Shield from seismic wide-angle reflection data. Canadian Journal of Earth Sciences. 37, pp. 439-458.

Miller, H. G., and Singh, V. 1994. Potential field tilt - a new concept for location of potential field sources: Journal of Applied Geophysics, 32, pp. 213-217.

Mints, M.V. 2017. The composite North American Craton, Superior Province: Deep crustal structure and mantle-plume model of Neoarchaean evolution. Precambrian Research 302, pp. 94–121.

Mortensen, J. K. 1993. U - Pb geochronology of the eastern Abitibi Subprovince. Part 1: Chibougamau - Matagami - Joutel region. Canadian Journal of Earth Sciences, 30, pp. 11-28.

Muir, T.L. 2013. Ontario Precambrian bedrock magnetic susceptibility geodatabase for 2001 to 2012; Ontario Geological Survey, Miscellaneous Release—Data 273 – Revised.

Naghizadeh, M., Snyder, D., Cheraghi, S., Foster, S., Cilensek, S., Floreani, E., Mackie, J., 2019. Acquisition and processing of wider bandwidth seismic data in crystalline crust: Progress with the Metal Earth Project. Minerals 2019, 9, pp. 145-158.

Nowell, D.A.G. 1999. Gravity terrain corrections - an overview; Journal of Applied Geophysics, 42, pp. 117-134.

Olaniyan, O.F., Smith, R.S., and Morris, W.M. 2013. Qualitative geophysical interpretation of the Sudbury Structure. Interpretation, 1, pp. 25-43.

Olaniyan, O.F., Smith, R.S., and Lafrance, B. 2014. A constrained potential field data interpretation of the deep geometry of the Sudbury structure; Canadian Journal of Earth Sciences, 51, pp. 715-729.

Percival, J. A., and Krogh, T. E. 1983. U-Pb zircon geochronology of the Kapuskasing structural zone and vicinity in the Chapleau- Foleyet area, Ontario. Canadian Journal of Earth Sciences, 20, pp. 830-843.

Pitcher, W. C. 1979. The nature, ascent and emplacement of granite magmas. Journal of the Geological Society of London, 136, pp. 627-662.

Pilkington, M., and P. Keating, 2010, Geologic application of magnetic data and using enhancement for contact mapping: 2010 EGM International Workshop, Expanded Abstract. pp. 1-5.

Racicot, D., Chown, E. H., and Hanel, T. 1984. Plutons of the Chibougamau-Desmaraisville belt: a preliminary survey. In Chibougamau-stratigraphy and mineralization. Edited by J. Guha and E. H. Chown. The Canadian Institute of Mining and Metallurgy, Special Volume 34, pp. 178-197.

Reid, A. B. 1980. Aeromagnetic survey design. Geophysics, 45, pp. 973-975.

Rivers, T., and Chown, E. H. 1986. The Grenville orogen in eastern Quebec and western Labrador: Definition, identification, and tectonometamorphic relationships of autochthonous, parautochthonous, and allochthonous terranes. In The Grenville Province. Edited by J. M. Moore, A. Davidson, and A. J. Baer. Geological Association of Canada, Special Paper 31, pp. 31-50.

Rivers, T., Martignole, J., Gower, C., and Davidson, A. 1989. New tectonic divisions of the Grenville Province, southeast Canadian Shield. Tectonics, 8, pp. 63-84.

Roest, W.R., Verhoef, J., and Pilkington, M. 1992, Magnetic interpretation using the 3-D analytic signal, Geophysics, 57, pp.116-125.

Sawyer, E.W., and Benn, K. 1993. Structure of the high-grade Opatica Belt and adjacent low-grade Abitibi Subprovince, Canada: An Archaean mountain front, Journal of Structural Geology, 15, pp. 1443-1458.

Sharma, K. M. N., Gobeil, A., and Mueller, W. l987. Stratigraphie de la région du Lac Caopatina. Ministère de 1'Energie et des Ressources du Québec, MB 87-16.

Scintrex Limited 2018. CG-6 Autograv™ gravity meter operation manual, https://scintrexltd.com/wp-content/uploads/2018/04/CG-6-Operations-Manual-RevB.pdf, 87p, [Date Accessed: 2nd March 2018].

Spector, A., and Grant, F.S. 1970. Statistical models for interpreting aeromagnetic data. Geophysics, 35, pp. 293-302.

Telford, W.M., Geldart, L.P., and Sheriff, R.E. 1990, Applied Geophysics. 2nd Edition, Cambridge University Press. 770p.

Telford, W.M., Geldart, L.P., Sheriff, R.E., and Keys, D.A., 1976, Applied Geophysics. Cambridge University Press, 860p.

Telmat, H., Mareschal, J.C., Gariepy, C., David, J., and Antonuk, C.N. 2000. Crustal models of the eastern Superior Province, Quebec, derived from new gravity data. Canadian Journal of Earth Sciences, 37, pp. 385-397.

Winardhi, S., and Mereu, R.F. 1997. Crustal velocity structure of the Superior and Grenville provinces of the southeastern Canadian Shield. Canadian Journal of Earth Sciences, 34, pp. 1167–1184.

Wynne-Edwards, H. R. 1972. The Grenville Province. In Variations in tectonic styles in Canada. Edited by R. A. Price and L. J. W. Douglas. Geological Association of Canada, Special Paper II, pp. 263-334.

Yushkin, V. 2011. Operating experience with CG5 gravimeters; Measurement Techniques, 54. pp.486-489.